Neuroscience and Biobehavioral Reviews 156 (2024) 105501

Contents lists available at ScienceDirect

Neuroscience and Biobehavioral Reviews

journal homepage: www.elsevier.com/locate/neubiorev

The effectiveness and safety of low-intensity transcranial ultrasound stimulation: A systematic review of human and animal studies

Penny Ping Qin [a], Minxia Jin [a,b], Adam Weili Xia [a], Ami Sinman Li [a], Tim Tianze Lin [a], Yuchen Liu [c], Rebecca Laidi Kan [a], Bella Bingbing Zhang [a], Georg S. Kranz [a,d,e,*]

[a] Department of Rehabilitation Sciences, The Hong Kong Polytechnic University, Hong Kong, SAR, China
[b] Shanghai YangZhi Rehabilitation Hospital (Shanghai Sunshine Rehabilitation Center), School of Medicine, Tongji University, Shanghai, China
[c] Department of Neuroimaging, Institute of Psychiatry, Psychology & Neuroscience, King's College London, London, UK
[d] Mental Health Research Center (MHRC), The Hong Kong Polytechnic University, Hong Kong, SAR, China
[e] Department of Psychiatry and Psychotherapy, Medical University of Vienna, Vienna, Austria

ARTICLE INFO

Keywords:
Low intensity
Focused ultrasound
Transcranial pulse stimulation
Transcranial ultrasound
Neuromodulation

ABSTRACT

Low-intensity transcranial ultrasound stimulation (LITUS) is a novel non-invasive neuromodulation technique. We conducted a systematic review to evaluate current evidence on the efficacy and safety of LITUS neuromodulation. Five databases were searched from inception to May 31, 2023. Randomized controlled human trials and controlled animal studies were included. The neuromodulation effects of LITUS on clinical or pre-clinical, neurophysiological, neuroimaging, histological and biochemical outcomes, and adverse events were summarized. In total, 11 human studies and 44 animal studies were identified. LITUS demonstrated therapeutic efficacy in neurological disorders, psychiatric disorders, pain, sleep disorders and hypertension. LITUS-related changes in neuronal structure and cortical activity were found. From histological and biochemical perspectives, prominent findings included suppressing the inflammatory response and facilitating neurogenesis. No adverse effects were reported in controlled animal studies included in our review, while reversible headache, nausea, and vomiting were reported in a few human subjects. Overall, LITUS alleviates various symptoms and modulates associated brain circuits without major side effects. Future research needs to establish a solid therapeutic framework for LITUS.

1. Introduction

Low-intensity transcranial ultrasound stimulation (LITUS) is a newly developed non-invasive brain stimulation (NIBS) technique that offers promising neuromodulation by acoustic energy transmitted into the brain parenchyma. LITUS typically reaches deeper brain regions with a high spatial resolution than transcranial magnetic stimulation (TMS) or transcranial electrical stimulation (TES), which sparks interest in the field (Fomenko et al., 2018). Unlike high-intensity transcranial focused ultrasound, which mediates brain function through thermal effects or ablation of diseased brain structure, LITUS aims to modulate neuronal activity through a non-thermal mechanism with minimal risk of tissue damage (Fini and Tyler, 2017; Tsui et al., 2005). Such a kind of neuromodulation through multiple ultrasound pulses is referred to as sonication in the LITUS literature.

LITUS has developed rapidly in recent years. In 2008, an ex vivo study first discovered the excitatory modulation effect of LITUS on neuronal activity and brain networks by using a low-intensity (temporal average intensity, I_{TA} <300 mW/cm^2), low-frequency (<0.65 MHz) ultrasonic stimulation (Tyler et al., 2008). Two years later, similar low-intensity, low-frequency ultrasound waves were applied to mouse brains through the skull, and ultrasound-elicited neuronal activity was detected in the motor cortex and hippocampus (Tufail et al., 2010). The first LITUS human study was conducted in 2013. Higher frequency (8 MHz), and low acoustic intensity (I_{TA} < 152 mW/cm^2) unfocused ultrasound was used to target the posterior frontal cortex in patients with chronic pain. The treatment group showed a significant improvement in mood compared to the placebo group (Hameroff et al., 2013). Since then, an increasing number of studies have emerged with extensive applications of LITUS in both animals and humans. However, to date, there is no guideline on the therapeutic use of LITUS. To establish the safety margin and to promote the therapeutic use of ultrasound as a NIBS

* Corresponding author at: Department of Rehabilitation Sciences, The Hong Kong Polytechnic University, Hong Kong, SAR, China.
E-mail address: georg.kranz@polyu.edu.hk (G.S. Kranz).

https://doi.org/10.1016/j.neubiorev.2023.105501
Received 26 September 2023; Received in revised form 7 November 2023; Accepted 2 December 2023
Available online 6 December 2023

technique, most studies determined the stimulated intensity based on the FDA recommendation for diagnostic ultrasound with spatial-peak temporal average intensity (I_{SPTA}) < 720 mW/cm^2 and spatial-peak pulse average intensity (I_{SPPA}) < 190 W/cm^2 (FDA, 2019), or based on the recommendation of the International Electro-technical Commission (IEC standard 60601–2–5) for physiotherapeutic ultrasound devices with I_{SPTA} < 3 W/cm^2 (Duck, 2007). Here, I_{SPPA} stands for the average pulse intensity at the spatial maximum position, relating to the short-term mechanical bio-effect. I_{SPTA} means the temporal average intensity at the spatial maximum position relating to the thermal bio-effect (Fomenko et al., 2018). In addition, LITUS has been classified into the following three types: (1) focused transcranial ultrasound stimulation (fTUS): performed with focused ultrasound transducers (Darmani et al., 2022); (2) unfocused transcranial ultrasound stimulation (unfocused TUS): performed with unfocused ultrasound transducers (Darmani et al., 2022); (3) transcranial pulse stimulation (TPS): performed with a device generating single ultrashort ultrasound pulses (3 μs) at frequencies of 1–5 Hz, with I_{SPTA} = 100 mW/cm^2 and I_{SPPA} = 111 W/cm^2 (Matt et al., 2022).

Previous systematic reviews summarized studies that revealed transcranial ultrasound stimulation effects on brain excitability and behavior (Sarica et al., 2022; Wang et al., 2019). However, the included studies had highly heterogeneous study designs, including randomized controlled design, within-subject design, uncontrolled design, and case reports, which limited the interpretation of this novel technique for its implementation in clinical and research settings. Moreover, within-subject studies with no adequate washout period were also included, which may introduce carryover effects, as compelling evidence showed that one LITUS session can induce a long-lasting neuromodulation effect for up to 40 min (Gibson et al., 2018; Hameroff et al., 2013; Zeng et al., 2022). Therefore, the present study aimed to systematically review and synthesize randomized controlled human trials and in vivo controlled animal studies to investigate the neuromodulation effects and side effects of LITUS.

2. Methods

This study followed the standards established in the Preferred Reporting Items for Systematic Reviews and Meta-Analysis (PRISMA) Statement (Page et al., 2021), and was registered on PROSPERO (CRD42023399150).

2.1. Search strategy

MEDLINE (via PubMed), Embase (via Embase), CENTRAL (in the Cochrane Library), CINAHL (via EBSCOHost), and WOS (via Web of Science) were searched from database inception to May 31, 2023. The language was limited to English and Chinese. The following keywords were used: “low intensity transcranial ultrasound”, “transcranial focused ultrasound”, “transcranial unfocused ultrasound”, “low intensity transcranial focused ultrasound”, “transcranial pulse stimulation”, “transcranial ultrasound”, “focused ultrasound”, “transcranial”, “ultrasound”, “neuromodulation”. See Supplementary Appendix 1 for the detailed search strategy. Reference lists of relevant reviews and included studies were searched to identify potential records.

2.2. Inclusion criteria and exclusion criteria

Studies were eligible for inclusion if they (1) were human studies with a randomized controlled design (including crossover design) or were controlled animal studies (inclusion was not limited to the randomized controlled design for animal studies as randomization in animal studies is not standardized) (Hooijmans et al., 2014); (2) used LITUS to modulate brain function through mechanical effect; here, we included studies that reported the use of low-intensity TUS or non-thermal TUS, or studies that used acoustic intensity that met FDA or IEC recommendations (Duck, 2007; FDA, 2019); (3) had a blank control group or sham control group; (4) had outcomes of interests including clinical or pre-clinical, neurophysiological, neuroimaging, histological and biochemical findings. Studies were excluded if they (1) used LITUS to open the blood-brain barrier in combination with microbubble injection for substances delivery; (2) conducted repeated measures without a washout time greater than 40 min.

2.3. Selection of studies and data extraction

Two reviewers (PQ & WLX) independently screened the titles and abstracts. The full text was assessed using inclusion and exclusion criteria. Any disagreements between the two reviewers were solved through discussion with the third reviewer (MXJ). Data was extracted by two independent reviewers (PQ & WLX) and recorded in a standardized form. The following information was extracted: (1) characteristics of subjects or animal models; (2) type of LITUS and control; (3) treatment parameters of LITUS (e.g. total intervention sessions, stimulation target and sonication parameters); (4) outcome measures; (5) main results of LITUS neuromodulation effects; (6) side effect of LITUS. Any disagreements between the two reviewers were solved through discussion with the third reviewer (MXJ).

2.4. Assessment of risk of bias in included studies

Two reviewers (PQ & WLX) independently assessed the risk of bias for each study. We used the Cochrane Risk of Bias 2 tool (Cochrane RoB 2.0) to assess the risk of bias for human studies, which comprises six domains: randomization process, period and carryover effects (applicable for crossover trials), deviations from the intended intervention, missing outcome data, measurement of the outcome, and selection of the reported result (Sterne et al., 2019). We used the Systematic Review Center for Laboratory Animal Experimentation Risk of Bias (SYRCLE's RoB) tool for animal experiments and assessed selection bias, performance bias, detection bias, attrition bias, reporting bias and other biases (Hooijmans et al., 2014). Any disagreements between the two reviewers were solved by consulting the third reviewer (MXJ).

2.5. Strategy for qualitative synthesis

Given the high heterogeneity of the included studies, it was not possible to perform meta-analyses (Cochrane, 2022). The neuromodulation outcomes of LITUS were categorized into four domains: clinical and pre-clinical, neurophysiological, neuroimaging, and histological and biochemical results. Studies with the same outcome of interest were grouped, and the comparative results between the LITUS group and the control group were summarized. In addition, the adverse effects associated with LITUS reported in individual studies were summarized.

3. Results

3.1. Study selection and study characteristics

The original search of the databases identified 1618 records and 180 studies were retrieved for full-text review. A total of 11 human studies and 44 animal studies were included in this systematic review. The study selection process is shown in Supplementary Figure 1. Studies excluded after full-text review were cited and the reasons for exclusion were explained in Supplementary Appendix 2.

Table 1 shows detailed characteristics of individual human studies. Eight of eleven human studies included healthy subjects, two studies included patients with depression, and one study included patients with chronic pain. Table 2 shows detailed characteristics of individual animal studies. Various disease models were used in animal studies, including Parkinson's disease (PD), depression, epilepsy, pain, ischemic brain

Table 1
Characteristics of included human studies.

Study	Type of subjects	Grouping (sample size)	Characteristics of LITUS			Main outcomes			Reported adverse effect
			Target	Stimulation sessions	Parameters	Outcome measures	Timepoint of outcome measurements	Main results (experimental group compared to the control group)	
Matt 2022	Healthy subjects	TPS; Sham; (n = 12 in the crossover study)	Left primary somatosensory cortex	4 min/ session; 3 sessions in consecutive 3 days	Pulse frequency: 4 Hz; Energy level: 0.25 mJ/ mm^2; I_{SPTA}: 100 mW/cm^2; I_{SPPA}: 111 W/cm^2; Number of pulses in a session: 1000; MI: 10.95	sMRI	Around 1 week after stimulation	No significant difference in grey matter volume between groups	sMRI did not reveal any signs of bleeding, edema, or other morphological alterations after the TPS and the sham TPS
						DTI		A decrease in axial diffusivity in the primary somatosensory cortex and primary motor cortex	
						Rs-fMRI		An increase in global efficiency in the left sensorimotor network	
Cheung 2023	Patients with major depression	TPS (n = 15); No TPS (n = 15)	Left dorsal lateral prefrontal cortex	1.25–1.6 min/ session; 3 sessions/ week for 2 weeks	Pulse frequency: 3–4 Hz; Energy level: 0.2–0.25 mJ/mm^2; I_{SPTA}: 100 mW/cm^2; I_{SPPA}: 111 W/ cm^2; Number of pulses in a session: 300; MI: 10.95	HDRS-17	At stimulation endpoint	A decrease in score	4% subjects reported headaches; One subject experienced nausea and vomiting
Badran 2020	Healthy subjects	fTUS; Sham; (n = 19 in the crossover study)	Right anterior thalamus	10 min/ session; 2 sessions in one day with a 10-min interval	F_0: 0.65 MHz; I_{SPTA}: 995 mW/ cm^2; I_{SPTA}: 719 mW/cm^2 (after the attenuation through the skull); I_{SPPA}: 19.9 W/cm^2; I_{SPPA}: 14.38 W/ cm^2 (after the attenuation through the skull); SD: 30 s; Trials of sonication: 10; ISI: 30 s; PRF: 10 Hz; PD: 5 ms; DC: 5%; Number of pulses in a sonication: 300; Peak rarefactional pressure 0.72 MPa; MI: 0.89	QST	At stimulation endpoint	An increase in thermal pain threshold	No adverse events were observed throughout the experiment
Samuel 2022	Healthy subjects	tb-fTUS; Sham; (n = 15 in the crossover study)	Left motor cortex	80 s/ session; 1 session	F_0: 0.5 MHz; I_{SPTA}: 230 mW/ cm^2; I_{SPPA}: 2.26 W/cm^2; SD: 80 s; PRF: 5 Hz; PD: 20 ms; DC: 10%; Number of pulses in a sonication: 400; Peak rarefactional pressure: NR; MI: NR	MEP induced by TMS	At stimulation endpoint	An increase in MEP amplitude	No subjects reported any adverse effects throughout the experiment
						SICI induced by TMS		A decrease in SICI	
						MEG		An increase in alpha spectral power in right sensorimotor/ frontal cortex and an increase in beta spectral power in right sensorimotor/ parieto-occipital cortex	

(continued on next page)

Table 1 (*continued*)

Study	Type of subjects	Grouping (sample size)	Characteristics of LITUS			Main outcomes			Reported adverse effect
			Target	Stimulation sessions	Parameters	Outcome measures	Timepoint of outcome measurements	Main results (experimental group compared to the control group)	
Sanguinetti 2020	Healthy subjects	fTUS (n = 24); Sham (n = 24)	Right inferior frontal gyrus	30 s/ session; 1 session	F_0: 0.5 MHz; I_{SPTA}: 130 mW/ cm^2; I_{SPPA}: 54 W/cm^2; I_{SPPA}: 16.2 W/cm^2 (after the attenuation through the skull); SD: 30 s; PRF: 40 Hz; PD: 0.065 ms; DC: 0.26%; Number of pulses in a sonication: 1200; Peak rarefactional pressure: 1.27 MPa; MI: 1.8	VAMS	10 min, 20 min, and 30 min after stimulation	An increase in global affect score 20 min and 30 min after stimulation	NR
Zeng 2022	Healthy subjects	tb-fTUS; Sham; (n = 15 in the crossover study)	Left motor cortex	80 s/ session; 1 session	F_0: 0.5 MHz; I_{SPTA}: 230 mW/ cm^2; I_{SPPA}: 2.26 W/cm^2; SD: 80 s; PRF: 5 Hz; PD: 20 ms; DC: 10%; Number of pulses in a sonication: 400; Peak rarefactional pressure: NR; MI: NR	MEP induced by TMS SICI induced by TMS ICF induced by TMS	5 min, 30 min, and 60 min after stimulation	An increase in MEP amplitude 5 min and 30 min after stimulation A decrease in SICI 5 min and 30 min after stimulation An increase in ICF 5 min after stimulation	No subjects reported any adverse effects throughout the experiments
	Healthy subjects	tb-fTUS; Sham; (n = 12 in the crossover study)	Left motor cortex	80 s/ session; 1 session	F_0: 0.5 MHz; I_{SPTA}: 230 mW/ cm^2; I_{SPPA}: 2.26 W/cm^2; SD: 80 s; PRF: 5 Hz; PD: 20 ms; DC: 10%; Number of pulses in a sonication: 400; Peak rarefactional pressure: NR; MI: NR	Visuomotor task	10 min after stimulation	A decrease in movement time	
Zhang 2022a	Healthy subjects	fTUS; Sham; (n = 20 in the crossover study)	Left motor cortex	10 min/ session; 1 session	F_0: 0.8 MHz; Intensity: 1.2 W/cm^2; SD: 1 s; Trials of sonication: 200; ISI: 2 s; PRF: NR; PD: NR; DC: NR; Number of pulses in a sonication: NR; Peak rarefactional pressure: NR; MI: NR	Finger tapping test MEP induced by TMS	At stimulation endpoint	An increase in score A decrease in MEP latency and an increase in MEP amplitude	No significant difference of discomfort score between groups
Reznik 2020	Patients with mild to moderate depression	fTUS (n = 12); Sham (n = 12)	Right frontal-temporal cortex	30 s/ session; 5 sessions in a week	F_0: 0.5 MHz; I_{SPTA}: 71 mW/ cm^2; I_{SPPA}: 14 W/cm^2; SD: 30 s; PRF: NR; PD: NR; DC: NR; Number of pulses in sonication: NR; Peak rarefactional	PSWQ	At stimulation endpoint	A decrease in score	NR

(*continued on next page*)

Table 1 (*continued*)

Study	Type of subjects	Grouping (sample size)	Characteristics of LITUS			Main outcomes			Reported adverse effect
			Target	Stimulation sessions	Parameters	Outcome measures	Timepoint of outcome measurements	Main results (experimental group compared to the control group)	
					pressure: 0.65 MPa; MI: 0.9				
Gibson 2018	Healthy subjects	unfocused TUS (n = 19); Sham (n = 21)	Left motor cortex	2 min/ session; 1 session	F_0: 1.53–3.13 MHz; I_{SPTA}: 132.85 mW/ cm^2; I_{SPPA}: 34.96 W/cm^2; SD: 2 min; PRF: NR; PD: NR; DC: < 1%; Number of pulses in a sonication: NR; Peak rarefactional pressure: 1.02 MPa; MI: 0.67	MEP induced by TMS	At stimulation endpoint and 6 min after stimulation	An increase in MEPs amplitude	No significant difference in abnormal sensation and mood between groups
Guerra 2021	Healthy subjects	unfocused TUS; Sham (n = 16 in the crossover study)	Brainstem	180 s/ session; 1 session	F_0: 1.75 MHz; I_{SPTA}: NR; I_{SPPA}: NR; SD: 180 s; PRF: NR; PD: NR; DC: NR; Number of pulses in a sonication: NR; Peak rarefactional pressure: 1.85 MPa; MI: 1.4	EMG	3 min after stimulation	An increase in conditioned R2 area in the superior colliculus stimulation group	No subjects reported adverse events or any skin sensation during or after stimulation
Hameroff 2013	Patients with chronic pain	unfocused TUS; Sham; (n = 31 in the crossover study)	Right/left frontal-temporal cortex	15 s/ session; 1 session	F_0: 8 MHz; I_{SPTA}: 152 mW/cm^2; I_{SPPA}: NR; SD: 15 s; PRF: NR; PD: NR; DC: NR; Number of pulses in a sonication: NR; Peak rarefactional pressure: 1.98 MPa; MI: 0.7	VAMS	10 min and 40 min after stimulation	An increase in global affect score	One subject experienced an exacerbation of the headache after stimulation

TPS: transcranial pulse stimulation; MI: mechanical index; sMRI: structural magnetic resonance imaging; DTI: diffusion tensor imaging; Rs-fMRI: resting state functional magnetic resonance imaging; HDRS-17: Hamilton depression rating scale-17; fTUS: focused transcranial ultrasound stimulation; F_0: fundamental frequency; I_{SPTA}: spatial peak temporal average intensity; I_{SPPA}: spatial peak pulse average intensity; SD: stimulation duration; ISI: inter stimulation interval; PRF: pulse repetition frequency; PD: pulse duration; DC: duty cycle; QST: quantitative sensory thresholding; tb-fTUS: theta-burst focused transcranial ultrasound stimulation; NR: not reported; MEP: motor evoked potential; TMS: transcranial magnetic stimulation; SICI: short-interval intracortical inhibition; MEG: magnetoencephalography; VAMS: Visual analog mood scale; ICF: intracortical facilitation; PSWQ: Penn state worry questionnaire; unfocused TUS: unfocused transcranial ultrasound stimulation; EMG: electromyography.

injury, demyelination, Alzheimer's disease (AD), attention deficit hyperactivity disorder (ADHD), traumatic brain injury (TBI), hypertension, schizophrenia, sleep disorder, addictive disorder, and essential tremor.

3.2. Risk of bias within included studies

According to Cochrane RoB 2, four of eleven human studies were rated as having an overall high risk of bias, six studies as having a moderate risk of bias, and one study as having a low risk of bias (Supplementary Figure 2 **A,** Supplementary Table S1). The 10-item SYRCLE's RoB tool was used to assess the quality of 44 animal studies. The item prevalence was rated as follows: "no" (3.9%), indicating a high risk of bias; "unclear" (58.5%), indicating insufficient details; "yes" (37.6%), indicating a low risk of bias (Supplementary Figure 2B**,** Supplementary Table S2).

The results of the risk of bias assessment for human and animal studies are summarized in Supplementary Figure 2. See Supplementary Table S1 and Supplementary Table S2 for the full criteria for each tool and a full breakdown for each study.

3.3. Neuromodulation effects of LITUS

The neuromodulation effects of LITUS were categorized under four domains: clinical and pre-clinical, neuroimaging, neurophysiological, and histological and biochemical outcomes. A Sankey diagram (Fig. 1) illustrates the main neuromodulation effects of LITUS in human subjects. Two sunburst charts (Fig. 2, Fig. 3) illustrate the main neuromodulation effects of LITUS in healthy animals and in disease models, respectively.

3.3.1. Clinical and pre-clinical outcomes

LITUS effects were investigated for a variety of clinical and pre-clinical outcomes, including pain, mood, motor function, cognitive functions, and others.

Regarding pain, one human study and two animal studies investigated the analgesic effects of fTUS. A study demonstrated that two

Table 2
Characteristics of included animal studies.

Study	Type of animals	Grouping (sample size)	Characteristics of LITUS			Outcomes			Reported adverse effect
			Target	Stimulation sessions	Parameters	Outcome measures	Timepoint of outcome measurements	Main results (Experimental group vs. control group)	
Chu 2023	Healthy rats	fTUS1, fTUS2, fTUS3, fTUS4 (n = 15 for each group); Sham (n = 15)	Left primary motor cortex	5 min/ session; 1 session	F_0: 0.7 MHz; I_{SPTA} (fTUS1): 0.014 mW/cm^2; I_{SPTA} (fTUS2): 0.338 mW/cm^2; I_{SPTA} (fTUS3): 3.038 mW/cm^2; I_{SPTA} (fTUS4): 12.15 mW/cm^2; I_{SPPA}: 0.175 mW/cm^2 (fTUS1); I_{SPPA}: 4.225 mW/cm^2 (fTUS2); I_{SPPA}: 37.975 mW/cm^2 (fTUS3); I_{SPPA}: 151.875 mW/cm^2 (fTUS4); SD: 5 min; PRF: 100 Hz; PD: 0.8 ms; DC: 8%; Number of pulses in a sonication: 30000; Peak rarefactional pressure: 2.5–67.8 kPa; MI: 0.003–0.081	MEPs induced by TMS	At stimulation endpoint and measured every 5 min for 30 min after stimulation	A decrease in MEP amplitude in the fTUS2 group 5, 10,15 min after stimulation; A decrease in MEP amplitude in the fTUS3 and fTUS4 group at all follow-up timepoints	GFAP immunohistochemical staining showed no obvious astrogliosis at or near the sonicated sites in brains
Daniels 2018	Healthy rats	fTUS1 (n = 7); fTUS2 (n = 15); Sham (n = 3)	Inferior colliculus region	52 s/ session; 1 session	fTUS 1: F_0: 0.23 MHz; I_{SPTA}: NR; I_{SPPA}: 2.3 W/cm^2 SD: 100 ms; Trials of sonication: 17; ISI: 2900 ms; PRF: NR; PD: NR; DC: NR; Number of pulses in a sonication: NR; Pressure: 39.7 kPa; MI: 0.083 fTUS 2: F_0: 0.23 mHz; I_{SPTA}: NR; I_{SPPA}: 4.6 W/cm^2; SD: 100 ms; Trials of sonication: 17; ISI: 2900 ms; PRF: NR; PD: NR; DC: NR; Number of pulses in a session: NR; Pressure: 79.3 kPa; MI: NR	EEG	Measured for 30 min within 2 h after stimulation; Measured once a week until recovery of AEP amplitude or up to 2 months after stimulation	A decrease in AEP amplitude in fTUS1 and fTUS2 groups	T2-weighted MR image, H&E staining and histological analyses showed no brain damage, edema, tissue damage, or inflammatory response
Folloni 2019	Healthy macaques	fTUS for amygdala (n = 4); fTUS for ACC (n = 3); No fTUS (n = 9)	Amygdala; ACC	40 s/ session; 1 session	F_0: 0.25 MHz; I_{SPTA}: 19.5 W/cm^2 (for amygdala); I_{SPPA}: 64.9 W/cm^2 (for amygdala); I_{SPTA}: 5.63 W/cm^2 (for ACC); I_{SPPA}: 18.8 W/cm^2(for ACC); SD: 40 s; PRF:	fMRI	At stimulation endpoint	A decrease in the amygdala activity coupling and ACC activity coupling	sMRI showed no evidence of transient edema after fTUS

(*continued on next page*)

Table 2 (*continued*)

Study	Type of animals	Grouping (sample size)	Characteristics of LITUS			Outcomes			Reported adverse effect
			Target	Stimulation sessions	Parameters	Outcome measures	Timepoint of outcome measurements	Main results (Experimental group vs. control group)	
					10 Hz; PD: 30 ms; DC: 30%; Number of pulses in a sonication: 400; Maximum pressure: 1.44 MPa (for amygdala); Maximum pressure: 0.78 MPa (for ACC); MI: 2.88 (for amygdala); MI: 1.56 (for ACC)				
Huang 2019	Healthy rats	fTUS (n = 22); No fTUS (n = 22)	Hippocampus	10 min/ session; 1 session per day for 10 days	F_0: 0.5 MHz; I_{SPTA}: 360 mW/cm^2; I_{SPTA}: 225 mW/cm^2 (after attenuation through skull); I_{SPPA}: 7.2 W/cm^2; I_{SPPA}: 5.1 W/cm^2(after attenuation through skull); SD: 10 min; PRF: 500 Hz; PD: 0.1 ms; DC: 5%; Number of pulses in a sonication: 300000; Peak rarefactional pressure: 0.42 MPa; Peak rarefactional pressure: 0.35 MPa (after attenuation through skull); MI: 0.59	Dendritic structure ESPC dynamics Levels of GluN2A Number of c-Fos positive neurons	At sonication endpoint	An increase in dendritic spine density of hippocampal neurons An increase in ESPC frequency An increase in GluN2A level in the hippocampus An increase in c-Fos positive neurons in hippocampus	H&E staining and Nissl staining showed no hemorrhaging and tissue damage in the cortex, hippocampus, and the brain regions exposed to the beam path
Huang 2021	Healthy mice	fTUS (n = 14); Sham (n = 14)	Cortex and hippocampus	4 h/ session; 1 session	F_0: 0.5 MHz; I_{SPTA}: 235 mW/cm^2 (after attenuation through skull); I_{SPPA}: 4.7 W/cm^2 (after attenuation through skull); SD: 1 s; Trials of sonication: 7200; ISI: 1 s; PRF: 500 Hz; PD: 0.1 ms; DC: 5%; Number of pulses in a sonication: 500; Peak rarefactional pressure: 0.34 MPa (after attenuation through skull); MI: 0.48	Number of c-Fos positive neurons Level of protein marker for autophagy	At stimulation endpoint	An increase in c-Fos positive neurons in cortex and hippocampus An increase in the ratio of LC3BII/LC3BI and a decrease in p62 level in the cortex and hippocampus	H&E staining and Nissl staining showed no hemorrhaging, tissue damage or neuron loss in the cortex and hippocampus
Kim 2013	Healthy rats	fTUS (n = 7); Sham (n = 7)	Thalamic area	40 min/ session; 1 session	F_0: 0.35 MHz; I_{SPTA}: 3 W/cm^2; I_{SPPA}: NR; SD: 300 ms; Trials of sonication: 1045; ISI: 2 s; PRF: 1 kHz; PD: 0.5 ms; DC: NR;	PET	During stimulation and up to one hour after stimulation	An increase in SUV at the center of sonication focus compared to the contralateral area	No abnormal behavior in all animals; H&E staining showed no tissue damage or hemorrhage associated with sonication in 2 selected rats

(*continued on next page*)

Table 2 (*continued*)

Study	Type of animals	Grouping (sample size)	Characteristics of LITUS			Outcomes			Reported adverse effect
			Target	Stimulation sessions	Parameters	Outcome measures	Timepoint of outcome measurements	Main results (Experimental group vs. control group)	
					Number of pulses in a sonication: 300; Peak rarefactional pressure: 0.43 MPa; MI: 0.73				
Kim 2015	Healthy rats	fTUS with various I_{SPPA} (n = 9–10); fTUS with various DC (n = 9–10); Sham (n = 8)	Visual cortex	150 s/ session; 1 session for each parameter	Various I_{SPPA} with 5% DC: F_0: 0.35 MHz; $I_{SPTA\text{-}max}$: 250 mW/cm^2; I_{SPPA}: 1, 3, 5 W/cm^2; SD: 150 s; PRF: 100 Hz; PD: 0.5 ms; Peak rarefactional pressure: NR; MI: NR Various DC with 3 W/cm^2 I_{SPPA}: F_0: 0.35 MHz; $I_{SPTA\text{-}max}$: 250 mW/cm^2; PRF: 20, 166 Hz; PD: 0.5 ms; DC: 1, 8.3%; Peak rarefactional pressure: NR; MI: NR	EEG	Measured every 150 s for 9 times including 3 times before stimulation, 1 time during stimulation, and 5 times after stimulation	A decrease in VEP magnitude during the stimulation with I_{SPPA} of 3 W/cm^2 and DC of 5%; An increase in VEP magnitude during the stimulation with DC of 8.3% and I_{SPPA} of 3 W/cm^2	NR
Min 2011b	Healthy rats	fTUS (n = 12); No fTUS (n = 10)	Thalamus	20 min/ session; 1 session	F_0: 0.65 MHz; I_{SPTA}: 175 mW/cm^2; I_{SPPA}: 3.5 W/cm^2; SD: 20 min; PRF: 100 Hz; PD: 0.5 ms; DC: 5%; Number of pulses in a sonication: 120000; Pressure: 0.35 MPa; MI: 0.43	Extracellular level of dopamine and serotonin	During stimulation and up to 100 min after stimulation	An increase in dopamine level in the frontal lobe during the 100 min after stimulation; An increase in serotonin level in the frontal lobe 80–100 min after sonication	NR
Mohammadjavadi 2022	Healthy sheep	fTUS (n = 6); Sham (n = 5)	Lateral geniculate nucleus	20 min/ session; 2 consecutive sessions	F_0: 0.55 MHz; I_{SPTA}: 2.8–9.57 mW/cm^2 (after attenuation through skull); I_{SPPA}: 19.3–63.8 W/cm^2 (after attenuation through skull); SD: 300 ms; Trials of sonication: 923; ISI: 1 s; PRF: 500 Hz; PD: NR; DC: NR; Number of pulses in a sonication: 150; Peak rarefactional pressure: 0.55–1.0 MPa (after attenuation through skull); MI: 0.74–1.35	EEG	During stimulation	A decrease in VEP amplitude	NR
Wang 2020a	Healthy rats	fTUS (n = 19); Sham (n = 5)	Motor cortex	132 s/ session; 1 session	F_0: 0.5 MHz; I_{SPTA}: 440 mW/cm$^{2;}$ I_{SPPA}: 1.1 W/cm^2; SD: 400 ms; Trials of sonication: 30; ISI: 4 s;	EEG	During the stimulation and up to 2.1 s after sonication	An increase in LFP amplitude during stimulation and lasted 1.4 s after stimulation	NR

(*continued on next page*)

Table 2 (*continued*)

Study	Type of animals	Grouping (sample size)	Characteristics of LITUS			Outcomes			Reported adverse effect
			Target	Stimulation sessions	Parameters	Outcome measures	Timepoint of outcome measurements	Main results (Experimental group vs. control group)	
					PRF: 1 kHz; PD: 0.4 ms; DC: 40%; Number of pulses in a sonication: 400; Peak rarefactional pressure: NR: MI: NR				
Wang 2021b	Healthy mice	fTUS (n = 14); Sham (n = 13)	Periaqueductal gray	20 min/ session; 1 session	F_0: 3.8 MHz; I_{SPTA}: 321 mW/cm^2; I_{SPTA}: 70 mW/cm^2 (after the attenuation through skull); I_{SPPA}: 642 mW/cm^2; I_{SPPA}: 140 mW/cm^2 (after the attenuation through skull); SD: NR; Trials of sonication: NR; ISI: NR; PRF: 1 kHz; PD: 0.5 ms; DC: 50%; Number of pulses in a sonication: NR; Peak rarefactional pressure: 136 kPa; Peak rarefactional pressure: 63.4 kPa (after the attenuation through skull); MI: 0.07	OFT	During the stimulation	An increase in the time spent moving at high speed and an increase in mean speed	The estimated elevated temperature was 0.002 °C; H&E and Nissl staining showed no brain tissue injury caused by fTUS
Yang 2012	Healthy rats	fTUS (n = 9); Sham (n = 9)	Thalamus	20 min/ session; 1 session	F_0: 0.65 MHz; I_{SPTA}: 175 mW/cm2; I_{SPPA}: 3.5 W/cm2; SD: NR; Trials of sonication: NR; ISI: NR; PRF: 100 Hz; PD: 0.5 ms; DC: 5%; Number of pulses in a sonication: NR; Peak rarefactional pressure: 0.35 MPa; MI: 0.43	Extracellular level of GABA	During stimulation and up to 100 min after stimulation	A decrease in GABA level in the frontal lobe over time after stimulation	H&E staining showed no hemorrhaging or tissue damage at the sonication focus or the tissue exposed to the beam path
Yoo 2011	Healthy rats	fTUS; No fTUS; (n = 15 in the crossover study)	Thalamus	20 min/ session; 1 session	F_0: 0.65 MHz; I_{SPTA}: 300 mW/cm^2; I_{SPPA}: 6 W/cm^2; SD: NR; Trials of sonication: NR; ISI: NR; PRF: 100 Hz; PD: 0.5 ms; DC: 5%; Number of pulses in a sonication: NR; Peak rarefactional pressure: 0.49 MPa; MI: 0.61	Emergence from anesthesia	After the stimulation	A decrease in the time to initiation of responses to an air puff to the eyes, hind-paw pinching, and voluntary movements of limbs	NR
Yoo 2018	Healthy rats	fTUS; Sham; (n = 11 in the crossover study)	Somatosensory area	10 min/ session; 1 session	F_0: 0.65 MHz; I_{SPTA}: 210 mW/cm^2; I_{SPPA}: 4.2 W/cm^2; SD: NR; Trials of sonication: NR; ISI: NR; PRF: 100	EEG	5–35 min after stimulation	Differential SEP features were evident and persisted beyond 35 min after stimulation	The estimated temperature rise of 0.0938 °C was negligible and could not cause thermal damage

(*continued on next page*)

Table 2 (*continued*)

Study	Type of animals	Grouping (sample size)	Characteristics of LITUS			Outcomes			Reported adverse effect
			Target	Stimulation sessions	Parameters	Outcome measures	Timepoint of outcome measurements	Main results (Experimental group vs. control group)	
					Hz; PD: 0.5 ms; DC: 5%; Number of pulses in a sonication: 60000; Peak rarefactional pressure: NR; MI: NR				
Zhao 2023	Healthy mice	fTUS (n = 6); Sham (n = 6)	Somatosensory cortex	25 min/ session; 1 session per day for 7 days	F_0: 1 MHz; I_{SPTA}: 430 mW/cm^2; I_{SPPA}: 8.6 W/cm^2; SD: 5 min; Trials of sonication: 3; ISI: 5 min; PRF: 1 Hz; PD: 50 ms; DC: 5%; Number of pulses in a sonication: 300; Pressure: 0.51 MPa; MI: 0.51	Whisker-dependent behavior test	At stimulation endpoint; 7, 14 days after stimulation	A better performance at stimulation endpoint	NR
	Healthy mice	fTUS (n = 6); Sham (n = 3)				The two-photon fluorescence imaging	At stimulation endpoint; 7, 14, and 21 days after stimulation	An increase in synaptic activity at the stimulation endpoint and after stimulation; An increase in number of spines and spines formation at stimulation endpoint	
Guo 2015	Healthy rats	fTUS; No fTUS; (n = 9 in total)	Somatosensory cortex	24 min/ session; 1 session	F_0: 0.5 MHz; I_{SPPA}: 2.155 W/cm^2; I_{SPTA}: 43, 57, 72 mW/cm^2; SD: 0.4–0.67 s; Trials of sonication: 12; ISI: 2 min; PRF: 1.5 kHz; PD: NR; DC: NR; Number of pulses in a sonication: 600, 800, 1000; Peak rarefactional pressure: NR; MI: NR	LSI	Measured from 4 s before stimulation to 16 s after stimulation	An increase in cerebral blood flow velocity immediately after the stimulation and maintained up to 12 s after stimulation	NR
	Rat models of ischemic brain injury	fTUS (n = 16); No fTUS (n = 16)	Ischemic cortex	60 min/ session with 360 trials	F_0: 0.5 MHz; I_{SPTA}: 86 mW/cm^2; I_{SPTA}: NR; SD: 0.4 s; Trials of sonication: 360; ISI: 10 s; PRF: 1.5 kHz; PD: NR; DC: NR; Number of pulses: 600; Peak rarefactional pressure: NR; MI: NR	Neurological severity score	48 h after stimulation	A decrease in score	
						Infarct volume		A decrease in infarct volume	
						Number of neutrophils		A decrease in neutrophils in lateral striatum and a part of ischemic cortex	
Niu 2020	Healthy mice	fTUS (n = 14); Sham (n = 18)	Nucleus accumbens	30 min/ session; 1 session per day for 5 days	F_0: 3.4 MHz; I_{SPTA}: mW/cm^2; I_{SPTA}:; SD: 1 s; Trials of sonication: 600; ISI: 2 s; PRF: 1 kHz; PD: 0.05 ms; DC: 5%; Number of pulses: 1000; Pressure: 304 kPa; MI: 0.75	Conditioned place preference test	At stimulation endpoint	A decrease in time spent on the stimulated side	The maximum temperature increased after fTUS was estimated to be less than 0.003 °C
		fTUS (n = 6); Sham (n = 6)				Level of GluA1, GluA2 and GluA3	7 days after stimulation	An increase in GluA1, and a decrease in GluA2 and GluA3 level in nucleus accumbens	
	Mouse models of morphine addiction	fTUS (n = 4); Sham (n = NR)	Nucleus accumbens	30 min/ session; 1 session per day for 5 days		Morphine-induced place preference test	After 2 days stimulation and after 5 days stimulation	A decrease in score of conditioned place preference test	
Yi 2022	Healthy mice	fTUS (n = 6); Sham (n = 6)	Prefrontal cortex	30 min/ session; 1 session	F_0: 0.5 MHz; I_{SPTA}: 5.05 W/cm^2; I_{SPPA}: 10.09 W/cm^2; SD: 60 s; PRF: 100 Hz; PD: 5 ms; DC: 50%; Number	Number of c-Fos positive neurons	At stimulation endpoint	An increase in c-Fos positive neurons in prefrontal cortex	H&E and Nissl staining showed no tissue damage

(*continued on next page*)

Table 2 (*continued*)

Study	Type of animals	Grouping (sample size)	Characteristics of LITUS			Outcomes			Reported adverse effect
			Target	Stimulation sessions	Parameters	Outcome measures	Timepoint of outcome measurements	Main results (Experimental group vs. control group)	
	Mouse models of depression	fTUS (n = 13); Sham (n = 10)	Prefrontal cortex		of pulses in a sonication: 6000; Peak rarefactional pressure: 0.62 MPa; MI:0.88	TST, FST, EPM Level of inflammatory factors	17.5 h after stimulation	A better performance in TST, FST and EPM A decrease in IL-6, IL-1β, TNF-α levels in prefrontal cortex	NR
Zhou 2019	Healthy rats	fTUS (n = 3); Sham (n = 3)	Motor cortex	40 min/ session; 1 session/ day for 7 days	F_0: 0.8 MHz; I_{SPTA}:76 mW/cm^2 (after attenuation through skull); I_{SPPA}:760 mW/cm^2 (after attenuation through skull); SD: 6 s; Trials of sonication: 150; ISI: 10 s; PRF: 100 Hz; PD: 1 ms; DC: 10%; Number of pulses in a sonication: 600; Peak rarefactional pressure: NR; MI: 0.1	Number of c-Fos positive neurons	At stimulation endpoint	A significant increase in c-Fos positive neurons in motor cortex	The estimated elevated temperature was less than 0.02 °C; H&E and Nissl staining showed no tissue damage or hemorrhage associated with fTUS
	Rat models of acute Parkinson's disease	fTUS (n = 8); Sham (n = 8)	Motor cortex			OFT, pole test Total SOD and GSH-PX level	During the stimulation period 1 day after stimulation	A better performance in OFT and pole test An increase in total SOD and GSH-PX in striatum	
Zhou 2021	Healthy rats	fTUS (n = 4); Sham (n = 4)	Subthalamic nucleus	30 min/ session; 1 session	F_0: 3.8 MHz; I_{SPTA}: 430 mW/cm^2; I_{SPPA}: 860 mW/cm^2; SD: 1 s; Trials of sonication: 360; ISI: 4 s; PRF: 1 kHz; PD: 0.5 ms; DC: 50%; Number of pulses in a sonication: 1000; Peak rarefactional pressure: 190 kPa; MI: 0.1	Number of c-Fos positive neurons	At stimulation endpoint	An increase in c-Fos positive neurons in subthalamic nucleus	H&E, Nissl and TUNEL staining showed no brain tissue injury was induced by fTUS
	Healthy rats	fTUS (n = 4); Sham (n = 4)	Primary visual cortex			Number of c-Fos positive neurons	At stimulation endpoint	An increase in c-Fos positive neurons in primary visual cortex	
	Mouse models of chronic Parkinson's disease	fTUS (n = 13); Sham (n = 12)	Subthalamic nucleus	30 min/ session; 2 sessions per week for 5 weeks		Rotarod test and, pole test Number of dopaminergic neurons TNF-α, IL-1β, COX-2, NF-κB levels Amount of microglia and astrocytes Iba1, GFAP, αSyn and iNOS levels SOD level	At treatment endpoint	A better performance in rotarod test and pole test An increase in dopaminergic neurons in SN A decrease in TNF-α, IL-1β, COX-2, NF-κB levels in SN and striatum A decrease in microglia and astrocytes in SN and striatum A decrease in Iba1, GFAP, αSyn and iNOS levels levels in SN and striatum An increase in SOD level in SN and striatum	
Baek 2018	Mouse models of ischemic brain injury	fTUS (n = 12); No fTUS (n = 12)	Lateral cerebellar nucleus	20 min/ session; 2 sessions with an interval of 20 min	F_0: 0.35 MHz; I_{SPTA}: 1.27 W/cm^2; I_{SPPA}: 2.54 W/cm^2; SD: 100 ms; Trials of sonication: 571; ISI: 2 s; PRF: 1 kHz; PD: 0.5 ms; DC: 50%; Number of pulses in a sonication: 100; Peak	Balance beam test, adhesive removal test Brain edema	At treatment endpoint and during the 4-week follow-up period 2 days after treatment	A better performance in balance beam test and adhesive removal test A decrease in brain edema in ipsilateral hemisphere	Histological analysis showed no sign of bleeding or tissue damage in the cerebellum in 3 healthy rats exposed to the same fTUS as the fTUS group

(*continued on next page*)

Table 2 (*continued*)

Study	Type of animals	Grouping (sample size)	Characteristics of LITUS			Outcomes			Reported adverse effect
			Target	Stimulation sessions	Parameters	Outcome measures	Timepoint of outcome measurements	Main results (Experimental group vs. control group)	
					rarefactional pressure: NR; MI: 0.54				
Cao 2022	Rat models of hypertension	fTUS (n = 7); No fTUS (n = 7)	Solitary tract nucleus	20 min/ session; 1 session per day for 2 months	F_0: 0.6 MHz; I_{SPTA}: 1.64 W/cm^2; I_{SPPA}: 3.28 W/cm^2; SD: 200 ms; Trials of sonication: 230; ISI: 5 s; PRF: 250 Hz; PD: 2 ms; DC: 50%; Number of pulses in a sonication: 50; Peak rarefactional pressure: 0.32 MPa; MI: 0.41	Blood pressure Number of c-Fos expressing neurons Blood plasma levels of hormones	During the treatment period During the treatment period At treatment endpoint	A decrease in blood pressure An increase in c-Fos expressing neurons in solitary tract nucleus A decrease in plasma level of Aldo, ANGII, ANF, and Cor	H&E staining, TUNEL assay, and Nissl staining showed no apparent morphological or cellular damage in rat brain tissue after 2 months of fTUS
Chen 2020	Rat models of epilepsy	fTUS1 (n = 6); fTUS2 (n = 15); fTUS3 (n = 6); fTUS4 (n = 7); fTUS5 (n = 22); Sham (n = 20)	Hippocampus and thalamus regions	600 s/ session for fTUS1, fTUS2, fTUS3, fTUS5; 100 s/ session for fTUS4; 1 session	fTUS1: F_0: 0.5 MHz; I_{SPTA}: 703 mW/cm^2; I_{SPPA}: 2.34 W/cm^2; SD: 600 s; PRF: 100 Hz; PD: 3 ms; DC: 30%; Number of pulses in a sonication: 60000 fTUS2: F_0: 0.5 M Hz; I_{SPTA}: 750 mW/cm^2; I_{SPPA}: 9.38 W/cm^2; SD: 600 s; PRF: 100 Hz; PD: 0.8 ms; DC: 8%; Number of pulses in a sonication: 60000 fTUS3: F_0: 0.5 M Hz; I_{SPTA}: 1.25 W/cm^2; I_{SPPA}: 4.17 W/cm^2; SD: 600 s; PRF: 100 Hz; PD: 3 ms; DC: 30%; Number of pulses in a sonication: 60000 fTUS4: F_0: 0.5 M Hz; I_{SPTA}: 2.812 W/cm^2; I_{SPPA}: 9.37 W/cm^2; SD: 100 s; PRF: 100 Hz; PD: 3 ms; DC: 30%; Number of pulses in a sonication: 10000 fTUS5: F_0: 0.5 M Hz; I_{SPTA}: 2.812 W/cm^2; I_{SPPA}: 9.37 W/cm^2; SD: 600 s; PRF: 100 Hz; PD: 3 ms; DC: 30%; Number of pulses in a	EEG	Measured from 5 min before injection of pentylenetetrazol to 30 min after stimulation	A decrease in the number of spikes in all fTUS groups 10–15 min after pentylenetetrazol injection; A decrease in the number of spikes in fTUS2 and fTUS5 groups 15–20 min after pentylenetetrazol injection; A decrease in power spectral density of entire spectrum and decreases in alpha and theta power spectral densities in fTUS5 group 10–15 min after pentylenetetrazol injection; A decrease in beta power spectral density in fTUS4 and fTUS5 groups 10–15 min after pentylenetetrazol injection; A decrease in gamma power spectral density in fTUS2, fTUS4, fTUS5 groups 10–15 min after pentylenetetrazol injection	No behavioral abnormalities were observed, and H&E staining and low-magnification images showed no obvious tissue damage or inflammation, in rats treated with fTUS under these exposure parameters

(*continued on next page*)

Table 2 (*continued*)

Study	Type of animals	Grouping (sample size)	Characteristics of LITUS			Outcomes			Reported adverse effect
			Target	Stimulation sessions	Parameters	Outcome measures	Timepoint of outcome measurements	Main results (Experimental group vs. control group)	
					sonication: 60000 For fTUS1–5 and sham fTUS: Peak rarefactional pressure: 0–0.53 MPa; MI: 0–0.75				
Feng 2021	Mouse models of acute neuropathic pain	fTUS1 (n = 6); fTUS2 (n = 6); Sham (n = 6)	ACC	15 min/ session; 1 session per day for 21 days	fTUS1: F_0: 3.7 MHz; I_{SPTA}: 1.598 W/cm^2; I_{SPPA}: 15.980 W/cm^2; SD: 0.4 s; Trials of sonication: 300; ISI: 2.6 s; PRF: 1.5 kHz; PD: 0.07 ms; DC: 10%; Number of pulses in a sonication: 600; Pressure: 690 kPa; MI: 0.36 fTUS2: F_0: 3.7 MHz; I_{SPTA}: 3.498 W/cm^2; I_{SPPA}: 34.982 W/cm^2; SD: 15 min; PRF: 1.5 kHz; PD: 0.07 ms; DC: 10%; Number of pulses in a sonication: 600;	Nociceptive test	During the treatment period and 4, 11, 18 days after treatment	An increase in mechanical withdrawal threshold in contralateral side in the fTUS1 group 11 days after treatment; An increase in mechanical withdrawal threshold in surgical side in the fTUS2 group during the follow-up period; An increase in mechanical withdrawal threshold and an increase in thermal withdrawal threshold in contralateral side in the fTUS2 group 4 days after treatment	H&E staining showed no abnormal findings in ACC after fTUS
	Mouse models of chronic neuropathic pain	fTUS2 (n = 12); Sham (n = 12)			Pressure: 950 kPa; MI: 0.49	Nociceptive test	During the treatment period and 3 days after treatment	An increase in mechanical withdrawal threshold in the surgical side during treatment period	
						Expression of genes	At treatment endpoint	A decrease in expression of Hnrnph1 and Hnrnpd	
Guo 2021	Mouse models of depression	fTUS (n = 8–9); Sham (n = 8–9)	NR	20 min/ session; 1 session per day for 22 days	F_0: 1.5 MHz; Intensity: 25 mW/cm^2; SD: NR; Trials of sonication: NR; ISI: NR; PRF: 1 kHz; PD: 0.2 ms; DC: 20%; Number of pulses in a sonication: NR; Peak rarefactional pressure: NR; MI: NR	SPT Doublecortin level	24 h after treatment	An increase in SPI An increase in doublecortin level in the hippocampus	NR
	Mouse models of demyelination	fTUS (n = 3–4); Sham (n = 3–4)				MBP level and NG2 level	24 h after treatment	An increase in MBP and NG2 levels in the corpus callosum	
Hakimova 2015	Mouse models of epilepsy	fTUS (n = 13); No fTUS (n = 10)	Hippocampus	30 s/ session; Many sessions per day in 5 h, for 35 days	F_0: 0.2 MHz; I_{SPTA}: NR; I_{SPPA}: NR; SD: 30 s; PRF: 500 Hz; PD: 1 ms; DC: 50%; Number of pulses in a sonication: 15000; Peak rarefactional pressure: NR; MI: NR	Sociability task, FST	During stimulation period (day 21 to day 35)	A better performance in sociability task and FST	NR
	Mouse models of epilepsy	fTUS (n = 7); No fTUS (n = 9)	Hippocampus	30 s/ session; Many sessions per day in 5 h, for 21 days		EEG	During the stimulation	An increase in latency to status epilepsy; A decrease in spike frequency during status epilepsy	

(*continued on next page*)

Table 2 (*continued*)

Study	Type of animals	Grouping (sample size)	Characteristics of LITUS			Outcomes			Reported adverse effect
			Target	Stimulation sessions	Parameters	Outcome measures	Timepoint of outcome measurements	Main results (Experimental group vs. control group)	
						EEG	Measured for 2 weeks after stimulation	A decrease in spontaneous recurrent seizure	
Min 2011a	Rat models of epilepsy	fTUS (n = 9); Sham (n = 9)	Thalamus	3 min/ session; 2 sessions with a 10-minute interval	F_0: 0.65 MHz; I_{SPTA}: 130 mW/cm^2; I_{SPPA}: 2.6 W/cm^2; SD: 3 min; PRF: 100 Hz; PD: 0.5 ms; DC: 5%; Number of pulses in a sonication: 18000; Peak rarefactional pressure: 0.27 MPa; MI: 0.33	EEG	During stimulation and up to 10 min after stimulation	A decrease in number of epileptic bursts after 1st session, during and after the 2nd session; A decrease in theta activity after the 2nd session	H&E staining and TUNEL assay showed no damage in the brain tissue in healthy rats subjected to the same experimental procedure as the fTUS group
						Racine score	At stimulation endpoint	A decrease in score	
Pang 2021	Aging mice	fTUS1 (n = 14); fTUS2 (n = 15); Sham (n = 15)	Ventromedial hypothalamic nucleus	15 min/ session; 1 session per day for two 14 days, with 2.5 months in between	fTUS1: F_0: 1 MHz; I_{SPTA}: 540 mW/cm^2; I_{SPPA}: 5.4 W/cm^2; SD: 1 s; Trails of sonication: 150; ISI: 5 s; PRF: 1 kHz; PD: 100 μs; DC: 10%; Number of pulses in a sonication: 1000; Peak rarefactional pressure: 0.13 MPa; MI: 0.13 fTUS2: F_0: 1 MHz; I_{SPTA}: 540 mW/cm^2; I_{SPPA}: 5.4 W/cm^2; SD: 1 s; Trails of sonication: 150; ISI: 5 s; PRF: 10 Hz; PD: 10 ms; DC: 10%; Number of pulses in a sonication: 100; Peak rarefactional pressure: 0.13 MPa; MI: 0.13	Grip strength	During the stimulation period and at stimulation endpoint	An increase in grip strength at stimulation endpoint in fTUS2 group	H&E staining showed no tissue damage or hemorrhaging in the hypothalamus after fTUS1 or fTUS2
						Level of apoptosis factors	At stimulation endpoint	A decrease in Bax and an increase in Bcl-2/Bax ratio in fTUS2 group	
						Level of NMDA receptors and inflammatory cytokines		A decrease in NMDAR2B level in fTUS1 and fTUS2 groups; A decrease in TNF, IL-1β in fTUS1 group	
Park 2021	Mouse models of Alzheimer's disease	fTUS (n = 6); Sham (n = 6)	Entire brain	2 h/ session (repeated in stimulation blocks of 10-s ON and 30-s OFF periods); 1 session per day for 2 weeks	F_0: 0.3 MHz; I_{SPTA}: 14.4 mW/cm^2; I_{SPPA}: 1.2 W/cm^2; SD: 200 ms; Trials of sonication: 10; ISI: 800 ms; PRF: 40 Hz; PD: 3 ms; DC: 12%; Number of pulses in a sonication: 8; Peak rarefactional pressure: NR; MI: NR	Aβ42 level	At treatment endpoint	A decrease in total Aβ42 level in the pre- and infra-limbic cortex	Perls' Prussian blue staining showed no significant difference in micro-bleeding between groups
						EEG	During the treatment period and at treatment endpoint	An increase in spontaneous gamma power at treatment endpoint	
Peng 2021	Rat models of TBI	fTUS (n = 15); No fTUS (n = 15)	Brain damage area (in the parietal lobe)	10 min/ session; 1 session per day for 10 days	F_0: 0.5 MHz; Intensity: 1.2 W/cm^2; SD: 400 ms; PRF: 1 Hz; PD: 0.5 ms; DC: 0.05%; Number of pulses in a sonication: 0.4; Peak	DWI	During the treatment period; At treatment endpoint	A decrease in ADC value during treatment period and at treatment endpoint; An increase in FA value at any timepoints	NR

(*continued on next page*)

Table 2 (*continued*)

Study	Type of animals	Grouping (sample size)	Characteristics of LITUS			Outcomes			Reported adverse effect
			Target	Stimulation sessions	Parameters	Outcome measures	Timepoint of outcome measurements	Main results (Experimental group vs. control group)	
					rarefactional pressure: NR; MI: NR	Neurological function score		An increase in neurological function score during the treatment period	
						Loss rate of Nissl body	At treatment endpoint	A decrease in loss rate of Nissl body	
Sharabi 2019	Rat models of essential tremor	fTUS (n = 13); Sham (n = 3)	Olivo-cerebellar system	52 s/ session; 1–3 sessions	F_0: 0.23 mHz; I_{SPTA}: NR; I_{SPPA}: 27.2 W/ cm^2; SD: 100 ms; Trials of sonication: 17; ISI: 2900 ms; PRF: NR; PD: NR; DC: NR; Number of pulses in a sonication: NR; Peak rarefactional pressure: NR; MI: NR	EMG	During stimulation and up to 5 min after stimulation or until tremor recovered	A decrease in tremor frequency during or after the sonication in 12 responding rats, with complete tremor suppression in 6 responding rats; A decrease in average tremor frequency of the responding rats compared to baseline	No signs of neurological damage or reduction in well-being in all rats; The MR images of all scanned rats showed no abnormalities, or signs of treatment-induced toxicity
Song 2022	Rat models of Parkinson's disease	fTUS (n = 4); No fTUS (n = 4)	Right striatum	25 min/ session; 1 session/ day; 5 days per week for 6 weeks	F_0: 1 MHz; I_{SPTA}: 528 mW/cm^2; I_{SPPA}: 10.56 W/cm^2; SD: 5 min; Trials of sonication: 3; ISI: 5 min; PRF: 1 Hz; PD: 50 ms; DC: 5%; Number of pulses in a sonication: 300; Peak rarefactional pressure: NR; MI: NR	Amount of astroglia and microglia, and level of IL-1β and p-NF-κB p65	At treatment endpoint	A decrease in astroglia and microglia and a decrease in IL-1β and p-NF-κB p65 levels in the substantia nigra pars compacta	H&E and Nissl staining showed no fTUS-induced brain tissue injury in healthy rats subjected to the same experimental procedure as the fTUS group
						GDNF level		An increase in GDNF level in the substantia nigra pars compacta	
						Amount of dopamine transporter		An increase in dopamine transporter in the substantia nigra pars compacta	
						ZO-1 and claudin-5 level		An increase in ZO-1 and claudin-5 level in the substantia nigra pars compacta	
Tsai 2022	Rat models of schizophrenia	fTUS (n = 8); No fTUS (n = 8)	3.0 mm posterior and 2.5 mm lateral to the bregma of the brain	25 min/ session; 1 session/ day for 5 days	F_0: 1 MHz; I_{SPTA}: 528 mW/cm^2; I_{SPPA}: 10.56 W/cm^2; SD: 5 min; Trials of sonication: 3; ISI: 5 min; PD: 50 ms; PRF: 1 Hz; DC: 5%; Number of pulses in a sonication: 300; Peak rarefactional pressure: NR; MI: NR	NOR, MWM	24 h after the treatment	A better performance in NOR and MWM	NR
						Level of calbindin and parvalbumin		An increase in hippocampal calbindin and parvalbumin level	
						Number of parvalbumin-positive and calbindin-positive cells		An increase in and parvalbumin-positive and calbindin-positive cells in cingulate cortex	
						BDNF level		A decrease in hippocampal BDNF level and an increase in BDNF level in prefrontal cortex	
Wang 2020b	Mouse models of Parkinson's disease	fTUS (n = 11); Sham (n = 6)	Subthalamic nucleus	5 min/ session; 1 session	F_0: 0.5 MHz; I_{SPTA}: 379.5 mW/cm^2; I_{SPPA}: 7.59 W/cm^2; SD: 50	EEG	5 min after stimulation	A decrease in power spectrum of LFPs in beta band;	NR

(*continued on next page*)

Table 2 (*continued*)

Study	Type of animals	Grouping (sample size)	Characteristics of LITUS			Outcomes			Reported adverse effect
			Target	Stimulation sessions	Parameters	Outcome measures	Timepoint of outcome measurements	Main results (Experimental group vs. control group)	
					ms; Trials of sonication: 286; ISI: 1 s; PRF: 1 kHz; PD: 0.05 ms; DC: 5%; Number of pulses in a sonication: 50; Maximum pressure: 0.39 MPa; MI: 0.55			A decrease in PACI of LFPs of beta/high gamma band and a decrease in PACI of LFPs of beta/ripple band	
Wang 2021a	Mouse models of ischemic brain injury	fTUS (n = 6); No fTUS (n = 6)	Ischemic hemisphere	10 min/ session; 1 session per day for 7 days	F_0: 0.5 MHz; I_{SPTA}: 60 mW/cm^2; I_{SPPA}: 120 mW/cm^2; SD: 300 ms; Trials of sonication: 360; ISI: 2.7 s; PRF: 1 kHz; PD: 0.5 ms; DC: 50%; Number of pulses in a sonication: 300; Peak rarefactional pressure: NR; MI: NR	Brain atrophy volume	At treatment endpoint	A decrease in brain atrophy volume	NR
						Neurological severity score		A decrease in neurological severity score	
						EBST, corner test		A better performance in EBST and corner test	
						Number of M2 microglia, level of IL-10 and IL-10R		An increase in M2 microglia and an increase in IL-10 and IL-10R levels	
Wang 2023a	Rat models of ADHD	fTUS (n = 6); No fTUS (n = 6)	Prefrontal cortex	15 min/ session; 1 session/ day; 6 days per week for 2 weeks	F_0: 0.5 MHz; I_{SPTA}: 468 mW/cm^2; I_{SPPA}: 9.36 W/cm^2; SD: 50 ms; Trials of sonication: 857; ISI: 1 s; PRF: 1 Hz; PD: 50 ms; DC: 5%; Number of pulses in a sonication: 0.05; Maximum pressure: 0.53 MPa; MI: 0.75	OFT, MYM, Y-maze spontaneous alternation test	1–4 days after the treatment	A better performance in OFT, MYM and Y-maze spontaneous alternation test	NR
						T-maze	During the treatment period	A higher percentage of correct choices from day 3 to day 12	
						EEG	During the treatment period; 1 day and 7 days after treatment	An increase in average of spike firing rates of all neurons on day 7, and 1 day, 7 days after treatment; A lower LFPs at theta bands and higher LFPs at beta bands 1 day and 7 days after treatment; Higher LFPs 7 days after treatment	
						BDNF level	At treatment endpoint	An increase in BDNF level	
Yang 2022	Rat models of demyelination	fTUS (n = 5); No fTUS (n = 5)	Demyelination lesion in the brain (CA1 region of the right hippocampus)	25 min/ session; 1 session per day for 5 days	F_0: 1 MHz; I_{SPTA}: 500 mW/cm^2; I_{SPPA}: 2.5 W/cm^2; SD: 5 min; Trials of sonication: 25 min; ISI: 5 min; PRF: 100 Hz; PD: 2 ms; DC: 20%; Number of pulses in a sonication: 30000; Peak rarefactional pressure: NR; MI: NR	Amount of remyelination fibers	At treatment endpoint	An increase in remyelination fibers in hippocampus	NR
						Number of astrocytes and microglia		A decrease in microglia and astrocytes in hippocampus	
						Microglial morphology		An increase in the ramified microglia and a decrease in the hypertrophic, dystrophic, rod-shaped and amoeboid microglia in hippocampus	

(*continued on next page*)

Table 2 (*continued*)

Study	Type of animals	Grouping (sample size)	Characteristics of LITUS			Outcomes			Reported adverse effect
			Target	Stimulation sessions	Parameters	Outcome measures	Timepoint of outcome measurements	Main results (Experimental group vs. control group)	
						Number of oligodendrocytes		A decrease in oligodendrocyte progenitor cells and an increase in mature oligodendrocytes in hippocampus	
						BDNF level		An increase in hippocampal BDNF level	
Yao 2022	Rat models of migraine	Pre-fTUS (n = 7); Post-fTUS (n = 7); No fTUS (n = 7)	Whole brain	15 min/ session; 1 session	F_0: 0.5 MHz; I_{SPTA}: 415 mW/cm^2; I_{SPPA}: 8.3 W/cm^2; SD: 15 min; PRF: 1 Hz; PD: 50 ms; DC: 5%; Number of pulses in a sonication: 900000; Peak-to-peak pressure: 0.5 MPa; MI: 0.71	Number of head scratches	Measured before, during and after stimulation for a total of 135 min	A decrease in the number of head scratches in the pre-fTUS group and the post-fTUS groups	NR
						LSI		No significant difference in average cerebral blood flow velocity between groups	
Yuan 2020	Mouse models of Parkinson's disease	fTUS (n = 8); Sham (n = 8)	Subthalamic nucleus	5 min/ session; 1 session per day for 2 weeks	F_0: 0.5 MHz; I_{SPTA}: 255 mW/cm^2; I_{SPPA}: 5.1 W/cm^2; SD: 50 ms; Trials of sonication: 286; ISI: 1 s; PRF: 1 kHz; PD: 0.05 ms; DC: 5%; Number of pulses in a sonication: 50; Maximum pressure: 0.39 MPa; MI: 0.55	Wire hanging test, OFT, FST	During the treatment period (day 1, 2, 3, 4, 7) and at treatment endpoint (day 14)	A better performance on day 4, day 7, and at treatment endpoint	NR
Zhang 2019	Rat models of depression	fTUS (n = 17); Sham (n = 16)	Left prelimbic cortex	15 min/ session; 1 session per day for 2 weeks	F_0: 0.5 MHz; I_{SPTA}: 4.55 W/cm^2; I_{SPPA}: 7.59 W/cm^2; SD: 400 ms; Trials of sonication: 265; ISI: 3 s; PRF: 1.5 kHz; PD: 0.4 ms; DC: 60%; Number of pulses in a sonication: 600; Spatial-peak temporal-peak pressure: 0.38 MPa; MI: 0.54	SPT, OFT	At treatment endpoint	A better performance in SPT and OFT	H&E staining showed no fTUS-induced brain tissue injury
						BDNF level		An increase in BDNF level in hippocampus	
Zhang 2022b	Rat models of pain	fTUS (n = 6); No fTUS (n = 6)	Periaqueductal gray	5 min/ session; 1 session	F_0: 0.65 MHz; I_{SPTA}: 691 mW/cm^2 (after attenuation through skull); SD: 5 s; Trials of sonication: 30; ISI: 5 s; PRF: 100 Hz; PD: 1 ms; DC: 10%; Number of pulses in a sonication: 500; Peak rarefactional pressure: 0.47 MPa (after	EEG	Measured before stimulation to 25 min after stimulation	A decrease in LFP intensity of delta, theta, beta, and gamma waves during stimulation	H&E staining showed no notable brain tissue injury

(*continued on next page*)

Table 2 (*continued*)

Study	Type of animals	Grouping (sample size)	Characteristics of LITUS			Outcomes			Reported adverse effect
			Target	Stimulation sessions	Parameters	Outcome measures	Timepoint of outcome measurements	Main results (Experimental group vs. control group)	
					attenuation through skull); MI: 0.58				
Zhu 2023	Mouse models of depression	fTUS (n = 11); Sham (n = 11)	Dorsal raphe nucleus	30 min/ session; 1 session per day for 3 weeks	F_0: 1.1 MHz; I_{SPTA}: 2.84 W/cm^2 (after attenuated through skull); I_{SPPA}: 5.68 W/cm^2 (after attenuated through skull); SD: 1 s; Trials of sonication: 900; ISI: 1 s; PRF: 1 kHz; PD: 0.5 ms; DC: 50%; Number of pulses in a sonication: 1000; Maximum pressure: 484 kPa; MI: 0.46	TST	At stimulation endpoint	A decrease in tail suspension immobility duration	H&E staining showed no brain tissue damage
						5-HT level		An increase in 5-HT level in dorsal raphe nucleus	
	Healthy mice	fTUS (n = 3); Sham (n = 3)	Dorsal raphe nucleus	30 min/ session; 1 session		Number of c-Fos positive neurons	1 h after stimulation	An increase in c-Fos positive neurons	
Wang 2023b	Healthy mice	unfocused TUS (n = 10); Sham (n = 10)	Motor cortex	25 min/ session; 1 session per day for 7 days	F_0: 0.5 MHz; I_{SPTA}: 466 mW/cm^2; I_{SPPA}: 9.3 W/cm^2; PRF: 1 Hz; SD: 5 min; Trials of sonication: 3; ISI: 5 min; PD: 50 ms; DC: 5%; Number of pulses in a sonication: 300; Pressure: 0.53 MPa; MI: 0.75	NREM sleep ratio, REM sleep ratio	During the stimulation period (day 1, day 3) and at stimulation endpoint (day 7)	An increase in NREM sleep ratio and a decrease in REM sleep ratio on day 3 and day 7	NR
						LFP changes in NREM sleep		An increase in power of delta bands on day 3 and day 7; A decrease in power of spindle bands on day 1, day 3 and day 7; A decrease in sample entropy of delta bands and an increase in sample entropy of spindle bands on day 7	
						LFP changes in REM sleep		A decrease in power of theta bands and an increase in sample entropy of theta bands on day 7; An increase in power of gamma bands and a decrease in sample entropy of gamma bands on day 3 and day 7	
	Healthy mice	unfocused TUS (n = 6); Sham (n = 6)	Hippocampus			LFP changes in NREM sleep	During the stimulation period (day 1, day 3) and at stimulation endpoint (day 7)	An increase in power of delta and spindle bands on day 3 and day 7	NR
						LFP changes in REM sleep		A decrease in power of theta and gamma bands on day 3 and day 7	
	Mouse models of sleep disorders	unfocused TUS (n = 6); Sham (n = 6)	Motor cortex			REM sleep ratio	During the stimulation period (day 1, day 3) and at stimulation endpoint (day 7)	A decrease in REM sleep ratio on day 7	NR
						LFP changes in REM sleep		A decrease in power of theta bands on day 3	

(*continued on next page*)

Table 2 (*continued*)

Study	Type of animals	Grouping (sample size)	Characteristics of LITUS			Outcomes			Reported adverse effect
			Target	Stimulation sessions	Parameters	Outcome measures	Timepoint of outcome measurements	Main results (Experimental group vs. control group)	
	Mouse models of sleep disorder	unfocused TUS (n = 6); Sham (n = 6)	Hippocampus			Total sleep time, LFP changes in NREM and REM sleep	During the stimulation period (day 1, day 3) and at stimulation endpoint (day 7)	No significant difference between groups	NR
	Mouse models of Alzheimer's disease with sleep disorder	unfocused TUS (n = 6); Sham (n = 6)	Motor cortex			Total sleep time	During the stimulation period (day 1, day 3) and at stimulation endpoint (day 7)	An increase in total sleep time on day 7	NR
						NREM sleep ratio, REM sleep ratio		A significant increase in NREM and REM sleep ratio on day 7	
						LFP changes in NREM sleep		An increase in power of delta bands and a decrease in sample entropy of delta bands on day 3 and day 7; A decrease in sample entropy of spindle bands on day 7	
						LFP changes in REM sleep		A decrease in power of theta bands and an increase in sample entropy of gamma bands on day 7; An increase in sample entropy of theta bands on day 3 and day 7	
Xu 2020	Mouse models of Parkinson's disease	unfocused TUS (n = 6); No unfocused TUS (n = 6)	NR	5 min/ session; 1 session per day for 10 days	F_0: 1 MHz; Intensity: 0.3 W/cm^2; SD: 5 min; PRF: NR; PD: NR; DC: 100%; Number of pulses in a sonication: NR; Peak rarefactional pressure: NR; MI: 1.43	Number of dopaminergic neurons	At treatment endpoint	An increase in dopaminergic neurons in the striatum	H&E staining showed no pathological difference between groups

fTUS: focused transcranial ultrasound stimulation; F_0: fundamental frequency; I_{SPTA}: spatial peak temporal average intensity; I_{SPPA}: spatial peak pulse average intensity; SD: sonication duration; PRF: pulse repetition frequency; PD: pulse duration; DC: duty cycle; MI: mechanical index; MEPs: motor evoked potentials; TMS: transcranial magnetic stimulation; GFAP: glial fibrillary acidic protein; NR: not reported; ISI: inter stimulation interval; EEG: electroencephalogram; AEP: auditory evoked potential; MR: magnetic resonance; H&E: hemetoxylin and eosin; ACC: anterior cingulate cortex; fMRI: functional magnetic resonance imaging; sMRI: structural magnetic resonance imaging; ESPCs: excitatory spontaneous postsynaptic currents; PET: positron emission tomography; SUV: standardized uptake value; VEP: visual evoked potential; LFP: local field potential; OFT: open field test; GABA: γ-aminobutyric acid; SEP: somatosensory evoked potential; LSI: Laser speckle imaging; TST: tail suspension test; FST: forced swimming test; EPM: elevated plus maze; IL-6: interleukin-6; IL-1β: interleukin-1β; TNF-α: tumor necrosis factor-α; SOD: superoxide dismutase; GSH-PX: glutathione peroxidase; COX-2: cyclooxygenase-2; NF-κB: nuclear factor κB; SN: substantia nigra; αSyn: α-synuclein; iNOS: inducible nitric-oxide synthase; TUNEL: terminal deoxynucleotidyl transferase-mediated nick end labeling; Aldo: aldosterone; ANGII: angiotensin II; ANF: atrial natriuretic factor; Cor: cortisol; SPT: sucrose preference test; SPI: sucrose preference index; MBP: myelin basic protein; NG2: neural/glial antigen 2; NMDA: N-methyl-D-aspartate; TBI: traumatic brain injury; DWI: diffusion weighted imaging; ADC: apparent diffusion coefficient; FA: fractional anisotropy; EMG: electromyography; p- NF-κB p65: phosphorylation of nuclear factor κB p65; GDNF: glial cell line-derived neurotrophic factor; ZO-1: zonula occludens-1; NOR: novel object recognition; MWM: Morris water maze; BDNF: brain derived neurotrophic factor; PACI: phase-amplitude coupling index; EBST: elevated body swing test; IL-10: interleukin-10; IL-10R: interleukin-10 receptor; ADHD: attention deficit hyperactivity disorder; MYM: modified Y-maze; 5-HT: 5-hydroxytryptamine; unfocused TUS: unfocused transcranial ultrasound stimulation; NREM: non-rapid eye movement; REM: rapid eye movement.

sessions of 10-minute fTUS in the right anterior thalamus reduced pain sensitivity in healthy subjects (Badran et al., 2020). Animal studies found that a 10-minute whole-brain fTUS (Yao et al., 2022) and a 21-day anterior cingulate cortex (ACC) fTUS (Feng et al., 2021) alleviated pain in rodent disease models. Notably, fTUS showed a differential impact on acute and chronic neuropathic pain (Feng et al., 2021). An online analgesic effect was found in chronic neuropathic pain, whereas an offline analgesic effect was found in acute neuropathic pain (Feng et al., 2021).

Regarding mood, four human studies and four animal studies investigated the antidepressive effects of LITUS. A 30-second right ventrolateral prefrontal cortex (VLPFC) fTUS in healthy subjects (Sanguinetti et al., 2020) and a 15-second frontal-temporal cortex unfocused TUS in patients with chronic pain (Hameroff et al., 2013) resulted in a short-term improvement in mood for 10–40 min after sonication. Another study performed five 30-second fTUS sessions on the right fronto-temporal cortex in depressed patients and observed that the trait worry was mitigated after treatment (Reznik et al., 2020). Notably, six TPS sessions on the left dorsolateral prefrontal cortex (DLPFC) reduced depressive symptoms in patients with depression (Cheung et al., 2023). Animal studies found that fTUS reduced depressive behavior by stimulating the medial prefrontal cortex (Yi et al., 2022), left prelimbic cortex (Zhang et al., 2019), dorsal raphe nucleus (Zhu et al., 2023), and hippocampus (Hakimova et al., 2015).

Two human studies and ten animal studies investigated the modulation effect of fTUS on motor function. Two studies in healthy subjects targeting the left primary motor cortex revealed improvements in movement speed on visuomotor tasks after 10-minute fTUS (Zhang et al., 2022a) and after 80-second theta-burst fTUS (tb-fTUS) (Zeng et al., 2022). The restoration of motor function was found in rodent disease models after sonication. Tail muscle strength, movement duration and distance, motor coordination, bradykinesia and balance disorders were improved in rodent PD models by administration of fTUS in the motor cortex (Zhou et al., 2019) and subthalamic nucleus (STN) (Yuan et al., 2020; Zhou et al., 2021). Motor function recovery was also seen in the rat models of TBI (Peng et al., 2021) and rodent models of ischemic stroke (Baek et al., 2018; Guo et al., 2015; Wang et al., 2021a) following ultrasound treatment. Ultrasound treatment was applied to the injured area of the brain, except for one study where sonication was directed to the lateral cerebellar nucleus (LCN) (Baek et al., 2018). In aging rats, 28 sessions of 10 Hz-fTUS administrated to the hypothalamic nucleus enhanced the grip strength (Pang et al., 2021). A short-term effect on reducing hyperactivity in rat models of ADHD was observed 2–4 days after 12 fTUS sessions targeting the prefrontal cortex (Wang et al., 2023a).

Five animal studies investigated the effect of fTUS on cognitive function. Healthy mice (Zhao et al., 2023), aging mice (Pang et al., 2021), and rodent disease models, including ADHD (Wang et al., 2023a), schizophrenia (Tsai et al., 2022) and epilepsy (Hakimova et al., 2015) were involved in the studies, where the stimulated targets varied. In summary, an improvement in cognitive function was shown after fTUS targeting the barrel cortex (a region of the somatosensory cortex in mice) (Zhao et al., 2023), the prefrontal cortex (Wang et al., 2023a), the hippocampus (Hakimova et al., 2015) and a brain area lying 3.0 mm posterior and 2.5 mm lateral to the bregma of the mouse brain (Tsai et al., 2022).

Other modulation effects of fTUS were demonstrated in individual animal studies. These effects included a reduction in epileptic behavior (Min et al., 2011a) by targeting the thalamus and downregulation of systolic blood pressure by targeting the solitary tract nucleus in rodent disease models (Cao et al., 2022); as well as induction of avoidance behavior by targeting nucleus accumbens in healthy mice and mouse models of addictive disorder (Niu et al., 2020), triggering of defensive behavior by targeting the periaqueductal gray (Wang et al., 2021b) and the facilitation of recovery from anesthesia by targeting thalamus (Yoo et al., 2011) in healthy rodents.

3.3.2. Neurophysiological outcomes

LITUS effects were investigated for a variety of neurophysiological outcomes by recording electromyography (EMG) and electroencephalography (EEG) and by measuring excitatory spontaneous postsynaptic currents.

Seven studies investigated the stimulation effect of LITUS by using EMG. Four out of five human studies evaluated motor cortical excitability after sonication by measuring the TMS-induced motor-evoked potentials (MEPs). fTUS (Zhang et al., 2022a), unfocused TUS (Gibson et al., 2018) and tb-fTUS (Samuel et al., 2022; Zeng et al., 2022) increased the MEPs after one sonication at the hotspot in the left primary motor cortex in healthy subjects. The excitatory effect lasted 6 min after unfocused TUS (Gibson et al., 2018) and 30 min after tb-fTUS (Zeng et al., 2022). The tb-fTUS protocol also attenuated TMS-induced short-interval intracortical inhibition (SICI) up to 30 min and facilitated TMS-induced intracortical facilitation (ICF) up to 5 min after sonication (Samuel et al., 2022; Zeng et al., 2022). A similar excitatory effect of unfocused TUS on the trigeminal blink reflex was found in the remaining human study in which the superior colliculus was stimulated, and EMG was recorded in the orbicularis oculi muscle induced by electrical stimulation in the supraorbital nerve (Guerra et al., 2021). In contrast, animal studies demonstrated a suppressive effect on TMS-induced MEPs after fTUS in the left primary motor cortex in healthy rats (Chu et al., 2023) and showed online inhibition of EMG signal in tremor muscles after fTUS in the olivo-cerebellar system in mouse models of essential tremor (Sharabi et al., 2019). Overall, LITUS exhibited bidirectional (excitatory or suppressive) neuromodulation effects measured using EMG.

Thirteen animal studies evaluated modulation the effect of LITUS using EEG. In healthy rats, a suppressive effect of fTUS on auditory evoked potentials (AEPs) (Daniels et al., 2018) and visual evoked potentials (VEPs) (Mohammadjavadi et al., 2022) was demonstrated by targeting the inferior colliculus and the lateral geniculate nucleus, respectively. Whereas one study revealed that the fTUS-induced VEP amplitude change was dose-dependent by targeting the visual cortex (Kim et al., 2015). While the I_{SPPA} of 3 W/cm^2 was constant, a duty cycle (DC) of 5% suppressed the VEPs and 8.3% DC facilitated the VEPs, and 1% DC had no effect on the VEP amplitude (Kim et al., 2015). fTUS was also found to modulate somatosensory evoked potentials (SEPs) by targeting the somatosensory cortex, and the differential SEP features persisted beyond 35 min after a 10-minute fTUS (Yoo et al., 2018). Moreover, an online excitatory effect of fTUS was found in the motor cortex by exhibiting higher local field potential (LFP) amplitudes (Wang et al., 2020a). Overall, studies in healthy animals examining LITUS effects using EEG showed an evident modulation of brain excitability, and the direction of the modulation (excitation or suppression) might be affected by the sonication parameters. Furthermore, animal studies found that LITUS reversed disease-related LFPs in several rodent disease models, including sleep-deprived models (Wang et al., 2023b), AD models (Park et al., 2021), PD models (Wang et al., 2020b), ADHD models (Wang et al., 2023a), pain models (Zhang et al., 2022b) and epilepsy models (Chen et al., 2020; Hakimova et al., 2015; Min et al., 2011a).

One animal study detected the fTUS-induced functional synaptic plasticity in healthy rats by recording excitatory spontaneous postsynaptic currents. The frequency of spontaneous excitatory postsynaptic current of hippocampal neurons increased after ten daily 10-minute fTUS sessions in the hippocampus (Huang et al., 2019).

3.3.3. Neuroimaging outcomes

LITUS effects were investigated for a variety of neuroimaging outcomes, including magnetic resonance imaging (MRI), magnetoencephalogram (MEG), positron emission tomography (PET), laser speckle image and two-photon fluorescence imaging.

One human study and two animal studies utilized MRI to investigate the modulatory effect of LITUS. Structural magnetic resonance imaging

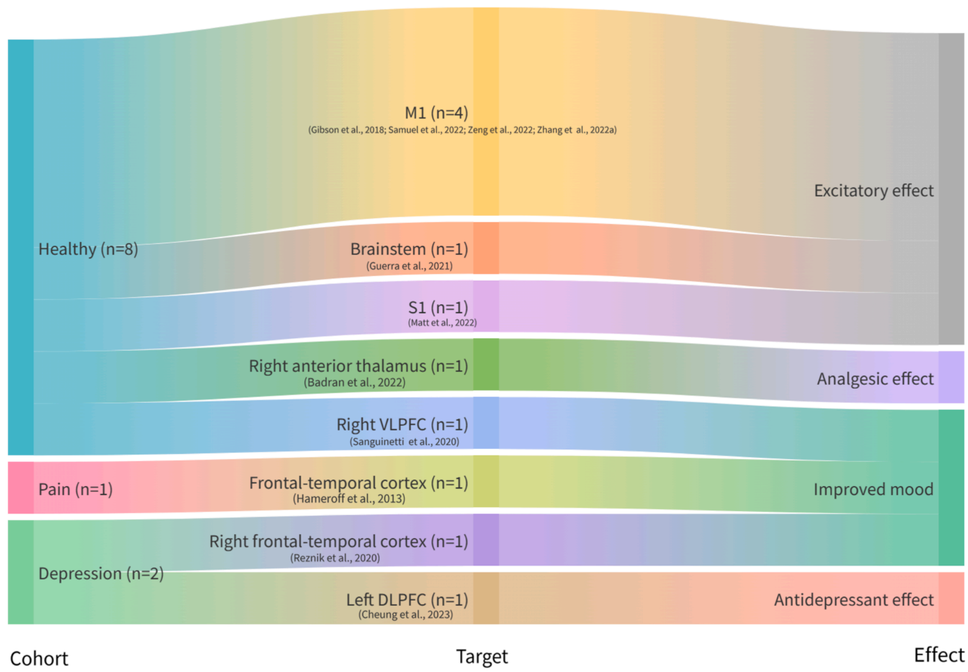

Fig. 1. Sankey diagram for main neuromodulation effects of LITUS in human subjects. Six human studies demonstrated an excitatory effect of LITUS in healthy subjects. Four out of six studies sonicated at the "hotspot" in the primary motor cortex, and the other two studies targeted the brainstem and primary somatosensory cortex, respectively. One study found a LITUS-induced analgesic effect in healthy subjects by stimulating the right anterior thalamus. Three studies discovered that LITUS improved mood in healthy subjects, patients with pain, and patients with depression, respectively, with one study targeting the ventrolateral prefrontal cortex and two studies targeting the frontal-temporal cortex. In addition, one study showed an antidepressant effect of LITUS at the left dorsolateral prefrontal cortex in depressed patients. M1: "hotspot" in primary motor cortex; S1: primary somatosensory cortex; VLPFC: ventrolateral prefrontal cortex; DLPFC: dorsolateral prefrontal cortex.

(sMRI), resting state functional MRI (rs-fMRI) and diffusion tensor imaging (DTI) were measured in healthy subjects after three sessions of TPS targeting the left primary somatosensory cortex (Matt et al., 2022). No change in grey matter volume was found in sMRI; whereas, rs-fMRI revealed an increase in functional connectivity in the left sensorimotor network one week after the last stimulation. Furthermore, DTI revealed decreased axial diffusivity in the primary somatosensory region and primary motor region after TPS. The authors claimed that the reduced axial diffusivity could indicate axonal formation. Rs-fMRI was also examined in an animal experiment but demonstrated a suppressive effect of fTUS on functional connectivity between the target areas (amygdala and ACC) and their interconnected areas in healthy macaques (Folloni et al., 2019). In Folloni's study, high I_{SPTA} of 19.5 W/cm^2 and 5.63 W/cm^2 were used, which could induce a possible thermal effect and result in reversible neuroinhibition (Darrow et al., 2019). In TBI rat models, DWI revealed a decrease in apparent diffusion coefficient and higher fractional anisotropy during the treatment period (Peng et al., 2021). The authors claimed that fTUS effectively reduced cerebral edema and white matter damage.

One human study applied MEG to assess oscillatory brain responses and network connectivity after tb-fTUS in the left motor cortex (Samuel et al., 2022). The results showed that tb-fTUS produced movement-associated changes in alpha and beta spectral power in distinct regions. Alpha spectral power decreased in the left limbic region, left cerebellum, bilateral sensorimotor cortices, and right supplementary motor area, while beta spectral power reduced prominently in the right parietal area and right basal ganglia. The authors concluded that the findings indicated the involvement of regions within motor networks in the response to tb-fTUS.

In an animal study on healthy rats, local glucose metabolism in the sonication target (thalamus) was examined using FDG (18-fludeoxyglucose) PET (Kim et al., 2013). After a 40-minute fTUS, higher local glucose metabolism was observed in the center of the sonication focus but not in other areas.

Two animal studies used laser speckle image to investigate the effect of fTUS on cerebral blood flow in rat models of pain (Yao et al., 2022) and healthy rats (Guo et al., 2015). After sonication with various numbers of tone bursts (600, 800, 1000), a rise of cerebral blood flow velocity was noticed immediately after fTUS at the ischemic cortex, and it maintained at a higher level up to 4–12 s after sonication, depending on the parameter (Guo et al., 2015). However, whole-brain fTUS did not alter cerebral blood flow velocity in the rat models of pain (Yao et al., 2022).

One animal study used two-photon fluorescence imaging in healthy rats. It showed that fTUS at the barrel cortex induced an enhancement in neuronal firing activity and an increase in the dendritic spine growth rate in the barrel cortex (Zhao et al., 2023).

3.3.4. Histological and biological outcomes

LITUS effects were studied for a variety of histological and biological outcomes involving anti-inflammatory responses, neurogenesis processes, antioxidant responses, and other disease-specific changes.

Seven animal studies examined the anti-inflammatory effect of fTUS in rodent disease models, including PD models (Song et al., 2022; Zhou et al., 2021), ischemic brain injury models (Guo et al., 2015; Wang et al., 2021a), aging models (Pang et al., 2021), depression models (Yi et al., 2022), and demyelination models (Yang et al., 2022). Reduction of inflammatory neurons such as astroglia and microglia (Song et al., 2022; Yang et al., 2022; Zhou et al., 2021), inflammatory cells such as neutrophils (Guo et al., 2015), and reduction of inflammatory cytokines (TNF-α, IL-1β) (Pang et al., 2021; Song et al., 2022; Yi et al., 2022; Zhou et al., 2021) and protein markers of neuroinflammation (COX-2, NF-κB) (Song et al., 2022; Zhou et al., 2021) were observed after fTUS at right striatum (Song et al., 2022), demyelination lesion area (Yang et al., 2022), subthalamic nucleus (Zhou et al., 2021), ischemic cortex (Guo et al., 2015), ventromedial hypothalamic nucleus (Pang et al., 2021),

Fig. 2. Sunburst chart for main neuromodulation effects of LITUS in healthy animals. The targets were noted in the inner rim boxes. Each target was given a number, and these numbers represent the number of studies in which the specific target was sonicated. The outer rim presents the main pre-clinical, neurophysiological, neuroimaging, histological, and biochemical outcomes of LITUS neuromodulation in healthy animals. ↑ means "increased"; ↓ means "decreased"; GABA: gamma-aminobutyric acid; DA: dopamine; 5-HT: 5-hydroxytryptamine; TMS-induced MEPs: transcranial magnetic stimulation-induced motor evoked potentials; LFPs: local field potentials; SEPs: sensory evoked potentials; AEPs: auditory evoked potentials; VEPs: visual evoked potentials.

and prefrontal cortex (Yi et al., 2022). On the other hand, an increment in anti-inflammatory M2 microglia and an increment in anti-inflammatory cytokines (IL-10 and IL-10R) were detected after fTUS at the ischemic hemisphere (Wang et al., 2021a).

Twelve animal studies investigated the neurogenesis effect of fTUS in rodent disease models and healthy rodents. LITUS increased levels of neurotrophic factors, including brain-derived neurotrophic factor (BDNF) and glial cell line-derived neurotrophic factor (GDNF), as well as expression of neurogenesis-related proteins in depression models (Guo et al., 2021; Zhang et al., 2019), PD models (Song et al., 2022; Xu et al., 2020), ADHD models (Wang et al., 2023a), and demyelination models (Yang et al., 2022), by targeting prelimbic cortex (Zhang et al., 2019), right striatum (Song et al., 2022), prefrontal cortex (Wang et al., 2023a), and demyelination lesion area (Yang et al., 2022). In a study on schizophrenia models, fTUS simultaneously reversed BDNF levels in the hippocampus and prefrontal cortex (Tsai et al., 2022). Furthermore, fTUS facilitated the remyelination process by increasing myelin basic protein (Guo et al., 2021; Yang et al., 2022) and the hippocampal fTUS activated hippocampal neurons by increasing dendritic spine density (Huang et al., 2019). LITUS also modulated the dopamine and GABA signaling pathways. Dopaminergic neurons (Xu et al., 2020; Zhou et al., 2021) and dopamine transporters (Song et al., 2022) in the substantia nigra increased in PD models following fTUS in subthalamic nucleus (Zhou et al., 2021) and right striatum (Song et al., 2022). In schizophrenia models, an increase in GABAergic neurons in the medial prefrontal lobe was detected 24 h after fTUS (Tsai et al., 2022). In healthy rats, extracellular dopamine levels in the frontal lobe increased up to 100 min after a 20-minute thalamic fTUS (Min et al., 2011b), while extracellular GABA levels declined (Yang et al., 2012). In healthy rodents, fTUS-induced increase in synaptic proteins was detected in target regions by stimulating the hippocampus (Huang et al., 2019) and nucleus accumbens (Niu et al., 2020). Moreover, fTUS activated the autophagy process in healthy mice by increasing the LC3BII/LC3BI ratio and decreasing p62 levels in the sonicated areas (cortex and hippocampus) (Huang et al., 2021). The authors speculated that fTUS had a neuroprotection effect on neurodegenerative diseases by increasing

Fig. 3. Sunburst chart for main neuromodulation effects of LITUS in animal disease models. The disease models were noted in the inner rim boxes. The targets were noted in the middle rim boxes. Each target was given a number, and these numbers represent the number of studies in which the specific target was sonicated. The outer rim presents the main pre-clinical, neurophysiological, neuroimaging, histological, and biochemical outcomes of neuromodulation of LITUS in animal disease models. ↑ means "increased"; ↓ means "decreased"; PD: Parkinson's disease; AD: Alzheimer's disease; TBI: traumatic brain injury; ADHD: attention deficit hyperactivity disorder; NR: no report; DN: dopaminergic neuron; 5-HT: 5-hydroxytryptamine; LFPs: local field potentials; EEG: electroencephalography; BDNF: brain-derived neurotrophic factor; BP: blood pressure.

self-digestion of abnormal constituents in obsolete cells. Taken together, fTUS demonstrated a neurogenesis effect on regulating the level of neurotrophic factors and neurogenesis-related proteins, facilitating the remyelination process, increasing the dendritic spine density of neurons, modulating dopamine and GABA signaling pathways, inducing the synaptic plasticity, and activating the autophagy process.

Three animal studies examined the antioxidant effect of fTUS in rodent PD models and aging models. Antioxidant enzymes comprising superoxide dismutase and glutathione peroxidase in the substantia nigra and striatum were increased, while inducible nitric-oxide synthase, one of the oxidant enzymes, was reduced after fTUS in PD models by targeting motor cortex (Zhou et al., 2019) and subthalamic nucleus (Zhou et al., 2021). In aging models, decreased expression in NMDA R2B receptors and reduced expression in the promotor of cell apoptosis (Bax) were observed after sonication at the ventromedial hypothalamic nucleus (Pang et al., 2021). Taken together, fTUS exhibited antioxidant effects by increasing antioxidant enzymes, decreasing oxidant enzymes, and inhibiting the age-related apoptosis process.

Eight animal studies found disease-specific changes induced by fTUS. In rodent brain injury models, recovery in the injured area was shown after fTUS in the injured cortex (Guo et al., 2015; Peng et al., 2021; Wang et al., 2021a) and LCN (Baek et al., 2018). In mouse models of AD, fTUS reduced total Aβ42 levels in the limbic cortex (Park et al., 2021). In mouse models of neuropathic pain, ACC-fTUS downregulated the highly expressed Hnrnph1 and Hnrnpd (Feng et al., 2021). In rat models of hypertension, a therapeutic effect of solitary tract nucleus-fTUS on reducing plasma levels of aldosterone (Aldo), angiotensin II (ANGII), endothelin (ET-1), atrial natriuretic factor (ANF) and cortisol (Cor) was found (Cao et al., 2022).

3.4. Adverse effects reported in the included studies

A total of 282 participants received LITUS in 11 human studies. Three fTUS studies (Badran et al., 2020; Samuel et al., 2022; Zeng et al., 2022), one unfocused TUS study (Guerra et al., 2021), and one TPS study (Matt et al., 2022) reported that no adverse events were observed throughout the experiment period. Two fTUS studies did not examine the adverse effects (Reznik et al., 2020; Sanguinetti et al., 2020). Two studies reported no significant difference in terms of discomfort or abnormal sensations between verum and sham groups, with one unfocused TUS study mentioning tingling as a common sensation (Gibson et al., 2018) and one fTUS study not mentioning any details (Zhang et al., 2022a). In a TPS study, headaches were reported in a few subjects (4%) and one subject complained of nausea and vomiting after the first treatment, but the symptoms resolved within 2 h without the necessity for medication and no further symptoms occurred (Cheung et al., 2023). Another unfocused TUS study reported that one subject experienced an exacerbation of headache after sonication, which subsided quickly without sequelae (Hameroff et al., 2013). In summary, no adverse events were reported in four fTUS studies; three unfocused and two TPS studies reported adverse events in 1% and 5% of subjects, respectively.

Of 44 animal experiments, 25 fTUS studies and one unfocused TUS study conducted safety evaluations by performing by H&E staining, Nissl staining, Perls' Prussian blue staining, TUNEL staining, glial fibrillary acidic protein immunohistochemical staining, thermal monitoring, MRI, and behavioral testing (Baek et al., 2018; Cao et al., 2022; Chen et al., 2020; Chu et al., 2023; Daniels et al., 2018; Feng et al., 2021; Folloni et al., 2019; Huang et al., 2019; Huang et al., 2021; Kim et al., 2013; Min et al., 2011a; Niu et al., 2020; Pang et al., 2021; Park et al., 2021; Sharabi et al., 2019; Song et al., 2022; Wang et al., 2021b; Xu et al., 2020; Yang et al., 2012; Yi et al., 2022; Yoo et al., 2018; Zhang et al., 2019; Zhang et al., 2022b; Zhou et al., 2021; Zhou et al., 2019; Zhu et al., 2023). None of them reported abnormal histological, biochemical, or behavioral findings after LITUS.

Regarding the mechanical index (MI), 36 out of 39 included studies (MI was not available in 16 included studies) utilized LITUS with MI < 1.9, while two human studies used TPS with an MI of 10.95 (Cheung et al., 2023; Matt et al., 2022) and an animal study used fTUS with an MI of 2.88 (Folloni et al., 2019)."

4. Discussion

In this review, we comprehensively summarized the neuromodulation effects of LITUS on clinical and pre-clinical, neurophysiological, neuroimaging, histological and biochemical outcomes in human and animal research. In the reviewed articles, the treatment effects were demonstrated in neurological disorders (including PD, AD, demyelination, epilepsy, brain injury, and essential tremor), psychiatric disorders (including depression, ADHD, schizophrenia, addictive disorder), pain, sleep disorders, and hypertension. LITUS also modulated pain threshold, improved mood and enhanced motor function in healthy subjects, and elicited defensive and avoidance behavior, improved cognitive function, modulated sleep rhythms, and facilitated awakening from anesthesia in healthy animals. LITUS-induced changes in neuronal excitability were found in the targeted areas and their connected regions, including the motor cortex, brainstem, hippocampus, olivo-cerebellar system, prefrontal cortex, visual cortex, inferior colliculus region, somatosensory cortex, periaqueductal gray, thalamus, amygdala, and anterior cingulate cortex. From a histological and biochemical point of view, LITUS modulated neurological function by regulating the anti-inflammatory reaction, neurogenesis process, antioxidant response, apoptosis process and autophagy process.

No histological, biochemical, or behavioral side effects were identified in the animal studies included in this review. In two human studies, reversible adverse events such as headache, nausea, and vomiting were described in a few subjects.

LITUS comprises fTUS, unfocused TUS and TPS. The mechanism of action of fTUS and unfocused TUS is similar. According to several hypotheses, ultrasonic waves interact with the intra- and extra- cellular environment through acoustic cavitation, acoustic radiation force and acoustic streaming, activating membrane gating kinetics, altering membrane capacitance, triggering synaptic transmission, and inducing NMDA-dependent synaptic plasticity (Brohawn et al., 2014; Chen et al., 2019; Jerusalem et al., 2019; Tyler, 2011; Shamli Oghli et al., 2023). Despite similar mechanisms, the different sonication parameters and the devices involved between fTUS and unfocused TUS could lead to different stimulation effects (Di Biase et al., 2019). Of note, the neuromodulation mechanism of TPS likely differs from fTUS and unfocused TUS, as TPS retains the intrinsic character of shockwaves. Low-energy extracorporeal shockwaves promote anti-inflammatory effects as well as the angiogenesis process and regeneration through mechanotransduction (d'd'd'Agostino et al., 2015). Studies revealed that the biological mechanism of low-energy extracorporeal shockwaves involves upregulation of BDNF and vascular endothelial growth factor (VEGB) (Hatanaka et al., 2016; Matsuda et al., 2020; Yahata et al., 2016) and facilitation of shifting endothelial nitrogen oxides to a tyrosine-dephosphorylated form, increasing NO production and suppressing nuclear-factor κB (Mariotto et al., 2005). Given the diversity of therapeutic modalities and different biomechanisms of LITUS, future research needs to specify the type of LITUS and the sonication parameters employed in studies, and investigate the neuromodulation effect of fTUS, unfocused TUS and TPS individually.

To establish a reliable therapeutic framework for LITUS, several issues need to be addressed. First, the investigation of the effective and safe dosage of acoustic waves to be delivered into the target is required. Various intensities of acoustic waves were applied in the included studies. In animal studies, I_{SPPA} from 120 mW/cm^2 to 64.9 W/cm^2 and I_{SPTA} from 0.014 mW/cm^2 to 19.5 W/cm^2 were used. In human studies, fTUS was performed using a range of I_{SPPA} values, ranging from 2.26 W/cm^2 to 14 W/cm^2, and I_{SPTA} values ranging from 71 mW/cm^2 to 995 mW/cm^2; unfocused TUS utilized an I_{SPPA} of 34.96 W/cm^2 and I_{SPTA} values ranging from 132.85 mW/cm^2 to 152 mW/cm^2; Regarding TPS, it employed an I_{SPPA} of 111 W/cm^2 and an I_{SPTA} of 100 mW/cm^2. Using too low ultrasound intensity may not be sufficient to exhibit a neuromodulation effect. An animal study showed that weak fTUS with 0.014 mW/cm^2 I_{SPTA} did not alter motor cortex excitability in healthy rats, while fTUS with 0.338–12.15 mW/cm^2 increased the cortex excitability (Chu et al., 2023). For humans, the lowest effective stimulation intensity should be higher, as 69–87% of ultrasound waves are attenuated by the human skull (Riis et al., 2022). Besides, the attenuation of acoustic waves at the skull increases with higher acoustic frequencies, therefore, unfocused TUS with a higher acoustic frequency can further diminish the sonication transmitted to the brain. On the other hand, the risk of mechanical and thermal damage to the brain increases with higher acoustic intensities. MI is commonly used to estimate the risk of mechanical damage caused by ultrasound, and an MI < 1.9 has been recommended by the FDA when using cephalic ultrasound devices (FDA, 2019). Based on current knowledge, there is no consensus on what intensity of LITUS is appropriate to guarantee robust neuronal effects while avoiding side effects. Simulation studies and in vitro studies can be performed prior to clinical trials to determine the appropriate dosage of ultrasound treatment. Second, the sonication parameters that mediate the treatment effect need to be clarified. Dose-response studies revealed that higher acoustic intensity increased the likelihood of motor responses (King et al., 2013) and that the magnitude of fTUS-induced VEPs increased with acoustic intensity (Lee et al., 2016). Furthermore, studies found that higher intensity fTUS had a stronger analgesic effect (Feng et al., 2021) and a stronger inhibitory effect on cortical excitability (Chu et al., 2023; Daniels et al., 2018). Aside from acoustic intensity, other sonication parameters such as pulse repetition frequency and pulse duration (Pang et al., 2021), number of tone bursts (Guo et al., 2015), duty cycle (Chen et al., 2020; Kim et al., 2015) and stimulation duration (Chen et al., 2020; Wang et al., 2020a) could influence the neuronal modulation effect. Specifically, Kim et al. (Kim et al., 2015) discovered that 5% DC combined with 3 W/cm^2 I_{SPPA} inhibited VEPs, whereas 8.3% DC combined with 3 W/cm^2 I_{SPPA} enhanced the VEPs amplitude. However, the factors that determine the bidirectional effect are uncertain. Further, a tb-fTUS with an 80-s sonication duration with 20-ms ultrasound pulses repeated every 200 ms (pulse repetition frequency: 5 Hz, DC: 10%, number of pulses: 400) was developed and demonstrated a superior excitatory effect compared to a conventional fTUS with the same intensity (Zeng et al., 2022). Third, proper target selection is critical for determining treatment outcomes of LITUS, given its highly region-specific nature (Folloni et al., 2019; Kim et al., 2013). Several potential targets were proposed in the included studies, including thalamus and ACC for pain modulation (Badran et al., 2020; Feng et al., 2021); DLPFC, medial prefrontal cortex, prelimbic cortex and dorsal raphe nucleus for treating depression (Cheung et al., 2023; Yi et al., 2022; Zhang et al., 2019; Zhu et al., 2023;); VLPFC and the right fronto-temporal cortex for improving mood (Reznik et al., 2020; Sanguinetti et al., 2020; Hameroff et al., 2013); motor cortex, the subthalamic nucleus and the lateral cerebellar nucleus for improving motor function (Zeng et al., 2022; Zhang et al., 2022a; Zhou et al., 2021; Yuan et al., 2020; Zhou et al., 2019; Baek et al., 2018). Fourth, a precise neuro-navigation should be prioritized when performing LITUS. Empirical localization using landmarks on the head may compromise the precision and efficacy of LITUS; hence, real-time neuro-navigation approaches such as MRI-guided (Badran et al., 2020) and optical tracking (Cheung et al., 2023; Matt et al., 2022) should be adopted.

Regarding the limitation of the current review, first, given the strict inclusion/exclusion criteria, some potentially important pilot studies were not included in the current review. Darmani et al. (2022) and Sarica et al. (2022) can be referred to for a summary of these studies. Second, we did not search for studies that exclusively investigated the adverse consequences of LITUS. The included randomized controlled human trials and controlled animal studies were insufficient to assess the occurrence of adverse events of LITUS (Peryer G et al., 2023). Third, the methodological quality of the included studies is not adequate. Ten out of eleven human studies have a moderate to high risk of bias. In 44 animal studies, most items in SYRCLE were rated as "unclear", suggesting that there is no sufficient detail to assess the potential risk of bias. Fourth, the high heterogeneity among studies on therapy modalities, stimulation targets, and sonication parameters affects the generalizability of the results. Therefore, the results of this study must be interpreted with caution.

5. Conclusions

LITUS is a promising non-invasive technique that modulates brain circuits in animals and humans. The neuromodulation effects induced by LITUS include altering neuronal excitability and regulating biochemical processes such as inflammatory responses and neurogenesis, which contribute to the improvement of clinical behavior and clinical symptoms and signs. No significant adverse events were identified in the included studies; however, reversible symptoms such as headache, nausea, and vomiting were reported in a few human subjects. Future research is required to investigate the optimal sonication parameters and treatment strategies using the precise target and real-time neuro-navigation technique.

Funding

The work was supported by the Mental Health Research Centre (Grant number: P0040786), the Strategic Hiring Scheme (Grant number: P0042417), and the Department of Rehabilitation Sciences (Grant number: P0043155), of The Hong Kong Polytechnic University to Georg S. Kranz.

Declaration of Competing interest

None.

Data Availability

Data will be made available on request.

Appendix A. Supporting information

Supplementary data associated with this article can be found in the online version at doi:10.1016/j.neubiorev.2023.105501.

References

Badran, B.W., Caulfield, K.A., Stomberg-Firestein, S., Summers, P.M., Dowdle, L.T., Savoca, M., Li, X., Austelle, C.W., Short, E.B., Borckardt, J.J., Spivak, N., Bystritsky, A., George, M.S., 2020. Sonication of the anterior thalamus with MRI-Guided transcranial focused ultrasound (tFUS) alters pain thresholds in healthy adults: a double-blind, sham-controlled study. Brain Stimul. 13, 1805–1812. https://doi.org/10.1016/j.brs.2020.10.007.

Baek, H., Pahk, K.J., Kim, M.J., Youn, I., Kim, H., 2018. Modulation of cerebellar cortical plasticity using low-Intensity focused ultrasound for poststroke sensorimotor function recovery. Neurorehabil Neural Repair 32, 777–787. https://doi.org/10.1177/1545968318790022.

Brohawn, S.G., Su, Z., MacKinnon, R., 2014. Mechanosensitivity is mediated directly by the lipid membrane in TRAAK and TREK1 K+channels. Proc. Natl. Acad. Sci. USA 111, 3614–3619. https://doi.org/10.1073/pnas.1320768111.

Cao, F., Zhang, J., Li, D., Wang, M., Lai, C., Xu, T., Bouakaz, A., Ren, P., Wan, M., Han, J., Zhang, S., 2022. Non-invasive ultrasound modulation of solitary tract nucleus exerts a sustainable antihypertensive effect in spontaneously hypertensive rats. IEEE Trans. Biomed. Eng. 70, 1869–1878. https://doi.org/10.1109/TBME.2022.3231343.

Chen, H., Garcia-Gonzalez, D., Jérusalem, A., 2019. Computational model of the mechanoelectrophysiological coupling in axons with application to neuromodulation. Phys. Rev. E 99, 032406. https://doi.org/10.1103/PhysRevE.99.032406.

Chen, S.G., Tsai, C.H., Lin, C.J., Lee, C.C., Yu, H.Y., Hsieh, T.H., Liu, H.L., 2020. Transcranial focused ultrasound pulsation suppresses pentylenetetrazol induced epilepsy in vivo. Brain Stimul. 13, 35–46. https://doi.org/10.1016/j.brs.2019.09.011.

Cheung, T., Li, T.M.H., Ho, Y.S., Kranz, G., Fong, K.N.K., Leung, S.F., Lam, S.C., Yeung, W.F., Lam, J.Y.T., Fong, K.H., Beisteiner, R., Xiang, Y.T., Cheng, C.P.W., 2023. Effects of transcranial pulse stimulation (TPS) on adults with symptoms of depression-A pilot randomized controlled trial. Int J. Environ. Res. Public Health 20, 2333. https://doi.org/10.3390/ijerph20032333.

Chu, P.C., Huang, C.S., Chang, P.K., Chen, R.S., Chen, K.T., Hsieh, T.H., Liu, H.L., 2023. Weak ultrasound contributes to neuromodulatory effects in the rat motor cortex. Int. J. Mol. Sci. 24, 2578. https://doi.org/10.3390/ijms24032578.

Cochrane, 2022. Cochrane handbook for systematic reviews of interventions version 6.3 (updated February 2022), in: Higgins JPT, T.J., Chandler J, Cumpston M, Li T, Page MJ, Welch VA (Ed.). Cochrane. Available from ⟨www.training.cochrane.org/handbook⟩.

d'Agostino, M.C., Craig, K., Tibalt, E., Respizzi, S., 2015. Shock wave as biological therapeutic tool: From mechanical stimulation to recovery and healing, through mechanotransduction. Int. J. Surg. 24, 147–153. https://doi.org/10.1016/j.ijsu.2015.11.030.

Daniels, D., Sharabi, S., Last, D., Guez, D., Salomon, S., Zivli, Z., Castel, D., Volovick, A., Grinfeld, J., Rachmilevich, I., Amar, T., Liraz-Zaltsman, S., Sargsyan, N., Mardor, Y., Harnof, S., 2018. Focused ultrasound-induced suppression of auditory evoked potentials in vivo. Ultrasound Med. Biol. 44, 1022–1030. https://doi.org/10.1016/j.ultrasmedbio.2018.01.010.

Darmani, G., Bergmann, T.O., Butts Pauly, K., Caskey, C.F., de Lecea, L., Fomenko, A., Fouragnan, E., Legon, W., Murphy, K.R., Nandi, T., Phipps, M.A., Pinton, G., Ramezanpour, H., Sallet, J., Yaakub, S.N., Yoo, S.S., Chen, R., 2022. Non-invasive transcranial ultrasound stimulation for neuromodulation. Clin. Neurophysiol. 135, 51–73. https://doi.org/10.1016/j.clinph.2021.12.010.

Darrow, D.P., O'Brien, P., Richner, T.J., Netoff, T.I., Ebbini, E.S., 2019. Reversible neuroinhibition by focused ultrasound is mediated by a thermal mechanism. Brain Stimul. 12, 1439–1447. https://doi.org/10.1016/j.brs.2019.07.015.

Di Biase, L., Falato, E., Di Lazzaro, V., 2019. Transcranial focused ultrasound (tFUS) and transcranial unfocused ultrasound (tUS) neuromodulation: From theoretical principles to stimulation practices. Front. Neurol. 10, 549 https://doi.org/10.3389/fneur.2019.00549.

Duck, F.A., 2007. Medical and non-medical protection standards for ultrasound and infrasound. Prog. Biophys. Mol. Biol. 93, 176–191. https://doi.org/10.1016/j.pbiomolbio.2006.07.008.

FDA, 2019. Marketing clearance of diagnostic ultrasound systems and transducers; Guidance for industry and food and drug administration staff. Available from ⟨https://www.fda.gov/regulatory-information/search-fda-guidance-documents/marketing-clearance-diagnostic-ultrasound-systems-and-transducers⟩.

Feng, X., Niu, L., Long, M., Luo, K., Huang, X., Chen, M., Lin, Z., Zhou, W., Yi, S., Ao, L., 2021. Transcranial ultrasound stimulation of the anterior cingulate cortex reduces neuropathic pain in mice. Evid. Based Complement. Altern. Med. 2021, 6510383 https://doi.org/10.1155/2021/6510383.

Fini, M., Tyler, W.J., 2017. Transcranial focused ultrasound: a new tool for non-invasive neuromodulation. Int. Rev. Psychiatry 29, 168–177. https://doi.org/10.1080/09540261.2017.1302924.

Folloni, D., Verhagen, L., Mars, R.B., Fouragnan, E., Constans, C., Aubry, J.F., Rushworth, M.F.S., Sallet, J., 2019. Manipulation of subcortical and deep cortical activity in the primate brain using transcranial focused ultrasound stimulation. Neuron 101, 1109–1116. https://doi.org/10.1016/j.neuron.2019.01.019.
Fomenko, A., Neudorfer, C., Dallapiazza, R.F., Kalia, S.K., Lozano, A.M., 2018. Low-intensity ultrasound neuromodulation: An overview of mechanisms and emerging human applications. Brain Stimul. 11, 1209–1217. https://doi.org/10.1016/j.brs.2018.08.013.
Gibson, B.C., Sanguinetti, J.L., Badran, B.W., Yu, A.B., Klein, E.P., Abbott, C.C., Hansberger, J.T., Clark, V.P., 2018. Increased excitability induced in the primary motor cortex by transcranial ultrasound stimulation. Front. Neurol. 9, 1007 https://doi.org/10.3389/fneur.2018.01007.
Guerra, A., Vicenzini, E., Cioffi, E., Colella, D., Cannavacciuolo, A., Pozzi, S., Caccia, B., Paparella, G., Di Stefano, G., Berardelli, A., Bologna, M., 2021. Effects of transcranial ultrasound stimulation on trigeminal blink reflex excitability. Brain Sci. 11, 645. https://doi.org/10.3390/brainsci11050645.
Guo, H., Baker, G., Hartle, K., Fujiwara, E., Wang, J., Zhang, Y., Xing, J., Lyu, H., Li, X. M., Chen, J., 2021. Exploratory study on neurochemical effects of low-intensity pulsed ultrasound in brains of mice. Med Biol. Eng. Comput. 59, 1099–1110. https://doi.org/10.1007/s11517-021-02351-9.
Guo, T., Li, H., Lv, Y., Lu, H., Niu, J., Sun, J., Yang, G.Y., Ren, C., Tong, S., 2015. Pulsed transcranial ultrasound stimulation immediately after the ischemic brain injury is neuroprotective. IEEE Trans. Biomed. Eng. 62, 2352–2357. https://doi.org/10.1109/TBME.2015.2427339.
Hakimova, H., Kim, S., Chu, K., Lee, S.K., Jeong, B., Jeon, D., 2015. Ultrasound stimulation inhibits recurrent seizures and improves behavioral outcome in an experimental model of mesial temporal lobe epilepsy. Epilepsy Behav. 49, 26–32. https://doi.org/10.1016/j.yebeh.2015.04.008.
Hameroff, S., Trakas, M., Duffield, C., Annabi, E., Gerace, M.B., Boyle, P., Lucas, A., Amos, Q., Buadu, A., Badal, J.J., 2013. Transcranial ultrasound (TUS) effects on mental states: a pilot study. Brain Stimul. 6, 409–415. https://doi.org/10.1016/j.brs.2012.05.002.
Hatanaka, K., Ito, K., Shindo, T., Kagaya, Y., Ogata, T., Eguchi, K., Kurosawa, R., Shimokawa, H., 2016. Molecular mechanisms of the angiogenic effects of low-energy shock wave therapy: roles of mechanotransduction. Am. J. Physiol. Cell Physiol. 311, C378–C385. https://doi.org/10.1152/ajpcell.00152.2016.
Hooijmans, C.R., Rovers, M.M., de Vries, R.B., Leenaars, M., Ritskes-Hoitinga, M., Langendam, M.W., 2014. SYRCLE's risk of bias tool for animal studies. BMC Med. Res. Method. 14, 43 https://doi.org/10.1186/1471-2288-14-43.
Huang, X., Lin, Z., Wang, K., Liu, X., Zhou, W., Meng, L., Huang, J., Yuan, K., Niu, L., Zheng, H., 2019. Transcranial low-intensity pulsed ultrasound modulates structural and functional synaptic plasticity in rat hippocampus. IEEE Trans. Ultrason Ferroelectr. Freq. Control 66, 930–938. https://doi.org/10.1109/TUFFC.2019.2903896.
Huang, X., Niu, L., Meng, L., Lin, Z., Zhou, W., Liu, X., Huang, J., Abbott, D., Zheng, H., 2021. Transcranial low-intensity pulsed ultrasound stimulation induces neuronal autophagy. IEEE Trans. Ultrason. Ferroelectr. Freq. Control 68, 46–53. https://doi.org/10.1109/TUFFC.2020.3028619.
Jerusalem, A., Al-Rekabi, Z., Chen, H., Ercole, A., Malboubi, M., Tamayo-Elizalde, M., Verhagen, L., Contera, S., 2019. Electrophysiological-mechanical coupling in the neuronal membrane and its role in ultrasound neuromodulation and general anaesthesia. Acta Biomater. 97, 116–140. https://doi.org/10.1016/j.actbio.2019.07.041.
Kim, H., Park, M.A., Wang, S., Chiu, A., Fischer, K., Yoo, S.S., 2013. PET/CT imaging evidence of FUS-mediated (18)F-FDG uptake changes in rat brain. Med. Phys. 40, 033501 https://doi.org/10.1118/1.4789916.
Kim, H., Park, M.Y., Lee, S.D., Lee, W., Chiu, A., Yoo, S.S., 2015. Suppression of EEG visual-evoked potentials in rats through neuromodulatory focused ultrasound. Neuroreport 26, 211–215. https://doi.org/10.1097/WNR.0000000000000330.
King, R.L., Brown, J.R., Newsome, W.T., Pauly, K.B., 2013. Effective parameters for ultrasound-induced in vivo neurostimulation. Ultrasound Med. Biol. 39, 312–331 (https://doi.org/).
Lee, W., Lee, S.D., Park, M.Y., Foley, L., Purcell-Estabrook, E., Kim, H., Fischer, K., Maeng, L.-S., Yoo, S.-S., 2016. Image-guided focused ultrasound-mediated regional brain stimulation in sheep. Ultrasound Med. Biol. 42, 459–470. https://doi.org/10.1016/j.ultrasmedbio.2012.09.009.
Mariotto, S., Cavalieri, E., Amelio, E., Ciampa, A.R., de Prati, A.C., Marlinghaus, E., Russo, S., Suzuki, H., 2005. Extracorporeal shock waves: from lithotripsy to anti-inflammatory action by NO production. Nitric Oxide 12, 89–96. https://doi.org/10.1016/j.niox.2004.12.005.
Matsuda, M., Kanno, H., Sugaya, T., Yamaya, S., Yahata, K., Handa, K., Shindo, T., Shimokawa, H., Ozawa, H., Itoi, E., 2020. Low-energy extracorporeal shock wave therapy promotes BDNF expression and improves functional recovery after spinal cord injury in rats. Exp. Neurol. 328, 113251 https://doi.org/10.1016/j.expneurol.2020.113251.
Matt, E., Kaindl, L., Tenk, S., Egger, A., Kolarova, T., Karahasanovic, N., Amini, A., Arslan, A., Saricicek, K., Weber, A., Beisteiner, R., 2022. First evidence of long-term effects of transcranial pulse stimulation (TPS) on the human brain. J. Transl. Med. 20, 26 https://doi.org/10.1186/s12967-021-03222-5.
Min, B.-K., Bystritsky, A., Jung, K.-I., Fischer, K., Zhang, Y., Maeng, L.-S., In Park, S., Chung, Y.-A., Jolesz, F.A., Yoo, S.-S., 2011a. Focused ultrasound-mediated suppression of chemically-induced acute epileptic EEG activity. BMC Neurosci. 12, 23 https://doi.org/10.1186/1471-2202-12-23.
Min, B.-K., Yang, P.S., Bohlke, M., Park, S., R.Vago, D., Maher, T.J., Yoo, S.-S., 2011b. Focused ultrasound modulates the level of cortical neurotransmitters: Potential as a new functional brain mapping technique. Int. J. Imaging Syst. Technol. 21, 232–240. https://doi.org/10.1002/ima.20284.
Mohammadjavadi, M., Ash, R.T., Li, N., Gaur, P., Kubanek, J., Saenz, Y., Glover, G.H., Popelka, G.R., Norcia, A.M., Pauly, K.B., 2022. Transcranial ultrasound neuromodulation of the thalamic visual pathway in a large animal model and the dose-response relationship with MR-ARFI. Sci. Rep. 12, 19588 https://doi.org/10.1038/s41598-022-20554-4.
Niu, L., Guo, Y., Lin, Z., Shi, Z., Bian, T., Qi, L., Meng, L., Grace, A.A., Zheng, H., Yuan, T. F., 2020. Noninvasive ultrasound deep brain stimulation of nucleus accumbens induces behavioral avoidance. Sci. China Life Sci. 63, 1328–1336. https://doi.org/10.1007/s11427-019-1616-6.
Page, M.J., Moher, D., Bossuyt, P.M., Boutron, I., Hoffmann, T.C., Mulrow, C.D., Shamseer, L., Tetzlaff, J.M., Akl, E.A., Brennan, S.E., Chou, R., Glanville, J., Grimshaw, J.M., Hróbjartsson, A., Lalu, M.M., Li, T., Loder, E.W., Mayo-Wilson, E., McDonald, S., McGuinness, L.A., Stewart, L.A., Thomas, J., Tricco, A.C., Welch, V.A., Whiting, P., McKenzie, J.E., 2021. PRISMA 2020 explanation and elaboration: Updated guidance and exemplars for reporting systematic reviews. BMJ 372, n160. https://doi.org/10.1136/bmj.n160.
Pang, N., Huang, X., Zhou, H., Xia, X., Liu, X., Wang, Y., Meng, W., Bian, T., Meng, L., Xu, L., Niu, L., 2021. Transcranial ultrasound stimulation of hypothalamus in aging mice. IEEE Trans. Ultrason Ferroelectr. Freq. Control 68, 29–37. https://doi.org/10.1109/TUFFC.2020.2968479.
Park, M., Hoang, G.M., Nguyen, T., Lee, E., Jung, H.J., Choe, Y., Lee, M.H., Hwang, J.Y., Kim, J.G., Kim, T., 2021. Effects of transcranial ultrasound stimulation pulsed at 40 Hz on Abeta plaques and brain rhythms in 5xFAD mice. Transl. Neurodegener. 10, 48 https://doi.org/10.1186/s40035-021-00274-x.
Peng, Y., Zhao, Y., Huang, Y., Liu, X., Zhang, H., Zhao, Z., Cheng, Y., Liu, L., 2021. Neuroprotective effects of low-intensity transcranial ultrasound stimulation combined with Baicalin intervention on traumatic brain injury in animals. Brain Res Bull. 175, 246–253. https://doi.org/10.1016/j.brainresbull.2021.07.028.
Peryer G, G.S., Junqueira, D., Vohra, S., Loke, Y.K., 2023. Adverse effects. In: Higgins, J. P.T., T.J., Chandler, J., Cumpston, M., Li, T., Page, M.J., Welch, V.A. (Eds.), Cochrane handbook for systematic reviews of interventions version 6.4 (updated August 2023). Cochrane (Available from ⟨www.training.cochrane.org/handbook⟩).
Reznik, S.J., Sanguinetti, J.L., Tyler, W.J., Daft, C., Allen, J.J.B., 2020. A double-blind pilot study of transcranial ultrasound (TUS) as a five-day intervention: TUS mitigates worry among depressed participants. In: Neurol Psychiatry Brain Res, 37, pp. 60–66. https://doi.org/10.1016/j.npbr.2020.06.004.
Riis, T.S., Webb, T.D., Kubanek, J., 2022. Acoustic properties across the human skull. Ultrasonics 119, 106591. https://doi.org/10.1016/j.ultras.2021.106591.
Samuel, N., Zeng, K., Harmsen, I.E., Ding, M.Y.R., Darmani, G., Sarica, C., Santyr, B., Vetkas, A., Pancholi, A., Fomenko, A., Milano, V., Yamamoto, K., Saha, U., Wennberg, R., Rowland, N.C., Chen, R., Lozano, A.M., 2022. Multi-modal investigation of transcranial ultrasound-induced neuroplasticity of the human motor cortex. Brain Stimul. 15, 1337–1347. https://doi.org/10.1016/j.brs.2022.10.001.
Sanguinetti, J.L., Hameroff, S., Smith, E.E., Sato, T., Daft, C.M.W., Tyler, W.J., Allen, J.J. B., 2020. Transcranial focused ultrasound to the right prefrontal cortex improves mood and alters functional connectivity in humans. Front Hum. Neurosci. 14, 52 https://doi.org/10.3389/fnhum.2020.00052.
Sarica, C., Nankoo, J.F., Fomenko, A., Grippe, T.C., Yamamoto, K., Samuel, N., Milano, V., Vetkas, A., Darmani, G., Cizmeci, M.N., Lozano, A.M., Chen, R., 2022. Human studies of transcranial ultrasound neuromodulation: A systematic review of effectiveness and safety. Brain Stimul. 15, 737–746. https://doi.org/10.1016/j.brs.2022.05.002.
Shamli Oghli, Y., Grippe, T., Arora, T., Hoque, T., Darmani, G., Chen, R., 2023. Mechanisms of theta burst transcranial ultrasound induced plasticity in the human motor cortex. Brain Stimul. 16, 1135–1143. https://doi.org/10.1016/j.brs.2023.07.056.
Sharabi, S., Daniels, D., Last, D., Guez, D., Zivli, Z., Castel, D., Levy, Y., Volovick, A., Grinfeld, J., Rachmilevich, I., Amar, T., Mardor, Y., Harnof, S., 2019. Non-thermal focused ultrasound induced reversible reduction of essential tremor in a rat model. Brain Stimul. 12, 1–8. https://doi.org/10.1016/j.brs.2018.08.014.
Song, W.S., Sung, C.Y., Ke, C.H., Yang, F.Y., 2022. Anti-inflammatory and neuroprotective effects of transcranial ultrasound stimulation on Parkinson's disease. Ultrasound Med Biol. 48, 265–274. https://doi.org/10.1016/j.ultrasmedbio.2021.10.001.
Sterne, J.A.C., Savović, J., Page, M.J., Elbers, R.G., Blencowe, N.S., Boutron, I., Cates, C. J., Cheng, H.-Y., Corbett, M.S., Eldridge, S.M., Emberson, J.R., Hernán, M.A., Hopewell, S., Hróbjartsson, A., Junqueira, D.R., Jüni, P., Kirkham, J.J., Lasserson, T., Li, T., McAleenan, A., Reeves, B.C., Shepperd, S., Shrier, I., Stewart, L.A., Tilling, K., White, I.R., Whiting, P.F., Higgins, J.P.T., 2019. RoB 2: a revised tool for assessing risk of bias in randomised trials. BMJ 366, l4898. https://doi.org/10.1136/bmj.l4898.
Tsai, C.W., Tsai, S.J., Pan, Y.J., Lin, H.M., Pan, T.Y., Yang, F.Y., 2022. Transcranial ultrasound stimulation reverses behavior changes and the expression of calcium-binding protein in a rodent model of schizophrenia. Neurotherapeutics 19, 649–659. https://doi.org/10.1007/s13311-022-01195-x.
Tsui, P.-H., Wang, S.-H., Huang, C.-C., 2005. In vitro effects of ultrasound with different energies on the conduction properties of neural tissue. Ultrasonics 43, 560–565. https://doi.org/10.1016/j.ultras.2004.12.003.
Tufail, Y., Matyushov, A., Baldwin, N., Tauchmann, M.L., Georges, J., Yoshihiro, A., Tillery, S.I.H., Tyler, W.J., 2010. Transcranial pulsed ultrasound stimulates intact brain circuits. Neuron 66, 681–694. https://doi.org/10.1016/j.neuron.2010.05.008.
Tyler, W.J., 2011. Noninvasive neuromodulation with ultrasound? A continuum mechanics Hypothesis. Neuroscientist 17, 25–36. https://doi.org/10.1177/1073858409348066.

Tyler, W.J., Tufail, Y., Finsterwald, M., Tauchmann, M.L., Olson, E.J., Majestic, C., 2008. Remote excitation of neuronal circuits using low-intensity, low-frequency ultrasound. PloS One 3, e3511. https://doi.org/10.1371/journal.pone.0003511.

Wang, J., Li, G., Deng, L., Mamtilahun, M., Jiang, L., Qiu, W., Zheng, H., Sun, J., Xie, Q., Yang, G.Y., 2021a. Transcranial focused ultrasound stimulation improves neurorehabilitation after middle cerebral artery occlusion in mice. Aging Dis. 12, 50–60. https://doi.org/10.14336/AD.2020.0623.

Wang, M., Wang, T., Ji, H., Yan, J., Wang, X., Zhang, X., Li, X., Yuan, Y., 2023a. Modulation effect of non-invasive transcranial ultrasound stimulation in an ADHD rat model. J. Neural Eng. 20, 16003. https://doi.org/10.1088/1741-2552/acb014.

Wang, P., Zhang, J., Yu, J., Smith, C., Feng, W., 2019. Brain Modulatory effects by low-intensity transcranial ultrasound stimulation (TUS): A systematic review on both animal and human studies. Front Neurosci. 13, 696 https://doi.org/10.3389/fnins.2019.00696.

Wang, T., Wang, X., Tian, Y., Gang, W., Li, X., Yan, J., Yuan, Y., 2023b. Modulation effect of low-intensity transcranial ultrasound stimulation on REM and NREM sleep. Cereb. Cortex 33, 5238–5250. https://doi.org/10.1093/cercor/bhac413.

Wang, X., Yan, J., Wang, Z., Li, X., Yuan, Y., 2020a. Neuromodulation effects of ultrasound stimulation under different parameters on mouse motor cortex. IEEE Trans. Biomed. Eng. 67, 291–297. https://doi.org/10.1109/TBME.2019.2912840.

Wang, Y., Niu, L., Meng, W., Lin, Z., Zou, J., Bian, T., Huang, X., Zhou, H., Meng, L., Xie, P., Zheng, H., 2021b. Ultrasound stimulation of periaqueductal gray induces defensive behaviors. IEEE Trans. Ultrason Ferroelectr. Freq. Control 68, 38–45. https://doi.org/10.1109/TUFFC.2020.2975001.

Wang, Z., Yan, J., Wang, X., Yuan, Y., Li, X., 2020b. Transcranial ultrasound stimulation directly influences the cortical excitability of the motor cortex in parkinsonian mice. Mov. Disord. 35, 693–698. https://doi.org/10.1002/mds.27952.

Xu, T., Lu, X., Peng, D., Wang, G., Chen, C., Liu, W., Wu, W., Mason, T.J., 2020. Ultrasonic stimulation of the brain to enhance the release of dopamine - A potential novel treatment for Parkinson's disease. Ultrason Sonochem. 63, 104955 https://doi.org/10.1016/j.ultsonch.2019.104955.

Yahata, K., Kanno, H., Ozawa, H., Yamaya, S., Tateda, S., Ito, K., Shimokawa, H., Itoi, E., 2016. Low-energy extracorporeal shock wave therapy for promotion of vascular endothelial growth factor expression and angiogenesis and improvement of locomotor and sensory functions after spinal cord injury. J. Neurosurg. Spine 25, 745–755. https://doi.org/10.3171/2016.4.Spine15923.

Yang, F.Y., Huang, L.H., Wu, M.T., Pan, Z.Y., 2022. Ultrasound neuromodulation reduces demyelination in a rat model of multiple sclerosis. Int J. Mol. Sci. 23, 10034. https://doi.org/10.3390/ijms231710034.

Yang, P.S., Kim, H., Lee, W., Bohlke, M., Park, S., Maher, T.J., Yoo, S.S., 2012. Transcranial focused ultrasound to the thalamus is associated with reduced extracellular GABA levels in rats. Neuropsychobiology 65, 153–160. https://doi.org/10.1159/000336001.

Yao, L., Chen, R., Ji, H., Wang, X., Zhang, X., Yuan, Y., 2022. Preventive and therapeutic effects of low-intensity ultrasound stimulation on migraine in rats. IEEE Trans. Neural Syst. Rehabil. Eng. 30, 2332–2340. https://doi.org/10.1109/TNSRE.2022.3199813.

Yi, S.S., Zou, J.J., Meng, L., Chen, H.M., Hong, Z.Q., Liu, X.F., Farooq, U., Chen, M.X., Lin, Z.R., Zhou, W., Ao, L.J., Hu, X.Q., Niu, L.L., 2022. Ultrasound stimulation of prefrontal cortex improves lipopolysaccharide-induced depressive-like behaviors in mice. Front Psychiatry 13, 864481. https://doi.org/10.3389/fpsyt.2022.864481.

Yoo, S.S., Kim, H., Min, B.K., Franck, E., Park, S., 2011. Transcranial focused ultrasound to the thalamus alters anesthesia time in rats. Neuroreport 22, 783–787. https://doi.org/10.1097/WNR.0b013e32834b2957.

Yoo, S.S., Yoon, K., Croce, P., Cammalleri, A., Margolin, R.W., Lee, W., 2018. Focused ultrasound brain stimulation to anesthetized rats induces long-term changes in somatosensory evoked potentials. Int J. Imaging Syst. Technol. 28, 106–112. https://doi.org/10.1002/ima.22262.

Yuan, Y., Zhao, Z., Wang, Z., Wang, X., Yan, J., Li, X., 2020. The Effect of low-intensity transcranial ultrasound stimulation on behavior in a mouse model of Parkinson's disease induced by MPTP. IEEE Trans. Neural Syst. Rehabil. Eng. 28, 1017–1021. https://doi.org/10.1109/TNSRE.2020.2978865.

Zeng, K., Darmani, G., Fomenko, A., Xia, X., Tran, S., Nankoo, J.F., Shamli Oghli, Y., Wang, Y., Lozano, A.M., Chen, R., 2022. Induction of human motor cortex plasticity by theta burst transcranial ultrasound stimulation. Ann. Neurol. 91, 238–252. https://doi.org/10.1002/ana.26294.

Zhang, D., Li, H., Sun, J., Hu, W., Jin, W., Li, S., Tong, S., 2019. Antidepressant-like effect of low-intensity transcranial ultrasound stimulation. IEEE Trans. Biomed. Eng. 66, 411–420. https://doi.org/10.1109/TBME.2018.2845689.

Zhang, M.F., Chen, W.Z., Huang, F.B., Peng, Z.Y., Quan, Y.C., Tang, Z.M., 2022a. Low-intensity transcranial ultrasound stimulation facilitates hand motor function and cortical excitability: A crossover, randomized, double blind study. Front Neurol. 13, 926027 https://doi.org/10.3389/fneur.2022.926027.

Zhang, T., Wang, Z., Liang, H., Wu, Z., Li, J., Ou-Yang, J., Yang, X., Peng, Y.B., Zhu, B., 2022b. Transcranial focused ultrasound stimulation of periaqueductal gray for analgesia. IEEE Trans. Biomed. Eng. 69, 3155–3162. https://doi.org/10.1109/TBME.2022.3162073.

Zhao, Z., Ji, H., Zhang, C., Pei, J., Zhang, X., Yuan, Y., 2023. Modulation effects of low-intensity transcranial ultrasound stimulation on the neuronal firing activity and synaptic plasticity of mice. Neuroimage 270, 119952. https://doi.org/10.1016/j.neuroimage.2023.119952.

Zhou, H., Niu, L., Xia, X., Lin, Z., Liu, X., Su, M., Guo, R., Meng, L., Zheng, H., 2019. Wearable ultrasound improves motor function in an MPTP mouse model of Parkinson's disease. IEEE Trans. Biomed. Eng. 66, 3006–3013. https://doi.org/10.1109/TBME.2019.2899631.

Zhou, H., Meng, L., Xia, X., Lin, Z., Zhou, W., Pang, N., Bian, T., Yuan, T., Niu, L., Zheng, H., 2021. Transcranial ultrasound stimulation suppresses neuroinflammation in a chronic mouse model of Parkinson's disease. IEEE Trans. Biomed. Eng. 68, 3375–3387. https://doi.org/10.1109/TBME.2021.3071807.

Zhu, Y., He, J., Wu, C., Wu, J., Cheng, Z., Chen, Y., Yuan, M., Zeng, L., Ji, X., 2023. Transcranial ultrasound stimulation relieves depression in mice with chronic restraint stress. J. Neural Eng. 20, 36011. https://doi.org/10.1088/1741-2552/ac8bfd.